Chapter 22

Compliant Robotics and Automation with Flexible Fluidic Actuators and Inflatable Structures

I. Gaiser, R. Wiegand, O. Ivlev, A. Andres, H. Breitwieser, S. Schulz and G. Bretthauer

Additional information is available at the end of the chapter

http://dx.doi.org/10.5772/51866

1. Introduction

The fields of Robotics and Automation have been experiencing a boom the last few years. According to the "International Federation of Robotics" (IFR) in 2011, 140,000 robot units have been sold. This made 2011 the year with the most robot sales ever [52, 55]. Experts predict a worldwide population of 1.3 million industrial robots until 2014. The prognoses for the field of service robotics are also very promising [53, 54, 56]. The growing number of service robots changes the general requirements for those robots. Whereas industrial robots are optimized regarding precision, repeatability, and reliability, requirements for service robots are different, due to more human-robot interaction (HRI) and operation in unstructured environments. This means these robots need to integrate new concepts in terms of adaptivity, safety, and universality, necessitating change in the characteristics of the actuation systems and the structures.

Safety strategies can be divided into pre-collision and post-collision strategies [75].

Post-collision strategies traditionally refer to the fields of measuring and control. The important questions in these fields are how human injury and robot damage can be minimized after a collision has occurred. Existing standards regarding robot safety [59, 60] are currently revised based on the most recent studies in the area of post-collision safety [12, 43–45].

Pre-Collision safety strategies have been discussed over the last 30 years [49, 67, 91, 93] including their limitations. More recent works discuss the fact that since the robots are operating in a human-centered environment, this must inform the design of the robots. Kathib et al. [68] describe how a robot should be designed to establish autonomous tasks as well as human guided tasks. Haegele et al. [46] determine that robots should either have a broad sensory infrastructure to limit forces and moments through measuring them, or should be inherently compliant. In 2006 Alami et al. [4] published a novel design paradigm for robots: **"design robots that are intrinsically safe and control them to deliver performance"**. In summary the requirements for a high degree of pre-collision safety are:

1. Lightweight
2. Inherent Compliance

These requirements are obvious in the field of service robotics since any interaction with animals, technology, or humans will be safer by implementing them. Operating industrial robots usually requires a strict division between the working area of the robot and the working area of the human, since industrial robots normally do not fulfill these requirements. However, there are many tasks that could be accomplished resulting in higher quality or more efficiency, with closer human-robot interaction.

A lower inertia of the robot allows faster operating speed. At the same time lower inertia reduces the impact in case of a collision. The application of composite materials can achieve this while maintaining stiffness and precision of the robot. An impressive example is the DLR "Lightweight Robotic Arm III" (LWR III) [50]. Another example presenting a robot for the manipulation of small masses is described in [75].

When looking at compliant actuation systems for robots it becomes clear that there is currently much effort to add compliance to conventional drives by adding elastic elements to the drive chain. This concept is referred to as series elastic actuation and has been carried out in many various forms [24, 121, 138, 140]. Other drives with more or less inherent compliance are piezo-drives, shape-memory-actuators (SMA), electrorheological drives, and polymeric actuators. Fluidic actuators are a well-suited actuation principle for compliant actuation. Whereas pneumatic actuators are already compliant because of the compressibility of gases, hydraulic actuators need the integration of compliant membrane structures in order to achieve compliance. This group of actuators is referred to as "Flexible Fluidic Actuators".

In addition to its drive elements a robot consists of structural elements connecting the drive elements. So independently from the drive system a robot can exhibit compliant characteristics via the integration of compliant structural elements.

2. Historical background

2.1. Flexible fluidic actuators

A Flexible Fluidic Actuator generally consists of a flexible shell that transmits potential energy, delivered by the pressurized fluid, into a mechanical force, which then can be used to create a motion.

The flexible fluidic operating principle has a strong background in biomimetics. Gutmann [41, 42] established the "Hydroskelett-Theorie" as an approach to explain evolutionary biology via the concepts of constructional morphology. He understood that the design-principles of hydrosceletts are responsible for the general designs of organisms. Gudo et al. [39, 40] developed this idea further by introducing the term "Engineering Morphology which describes how Gutmann's ideas can be applied to technical design. The biomimetic background of flexible fluidic actuation was specifically discussed in [11, 130]. These works discuss several examples on weevils and spiders and describe how crucial the membrane properties are regarding efficiency and durability of the whole actuation system. The transfer of the evolutionary optimized flexible fluidic drives developed by nature into powerful technical systems is one focus of this work.

A useful classification of Flexible Fluidic Actuators can be made according to their operating principle, or the kind of force they are creating. Here we differentiate between designs that use expansion, contraction or bending directions to drive a system.

2.1.1. Flexible fluidic "Expansion" actuators

The history of this group of actuators starts with simple designs for lifting applications [32, 90, 133, 136]. Current "lifting bags" are mainly used for rescue operations [134]. However, the biggest group of expansion actuators is air-springs or damping elements [17]. These systems are either bellow-type actuators or rolling lobe-type actuators. The first rolling lobe systems were developed in the 19th century [77] but the principle is still popular today. Some differences between types of air springs are depicted in figure 1.

Bellow-type actuators are suitable drives for application in harsh environments since there is no friction and they can compensate or create tilt motions up to 30° without any additional transmission elements. The smallest commercially available bellow-type actuators have a diameter of 160 mm. The following patents [10, 31, 37, 80, 96] give an idea as to how these air actuators have developed throughout the last century. However, these patents only describe the general design. Newer patents discuss problems concerning fatigue of the elastomer as well as the connectors [107].

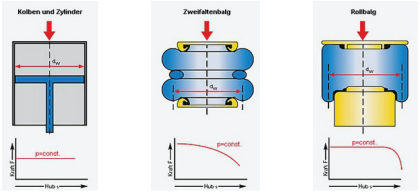

(a) Conventional Cylinder (b) Bellow-Type Actuator (c) Rolling Lobe-Type Actuator

Figure 1. Comparison of Different Kinds of Expansion Actuators [17]

Another big group is expansion actuators that work as rotary drive elements. [119] describes a solution where the structural integrity is created by the housing and the torque is created by an internal bellow-type actuator (figure 2(a))

The design proposed in [62] describes a bellow-type actuator suitable for linear or rotary motions as well as single chamber actuators (figure 2(b)-2(d)). The proposed materials for the bellow include rubbers as well as metals.

A very interesting design is introduced in [13]. The patent refers to fabrication techniques used in the tire industry and describes a layered membrane design with several reinforcement layers (figure 2(e), 2(f)).

[23] discusses the stress distribution in the membrane of a rotary actuator and requirements for achieving low bending stiffness and high tensile strength. Another approach is described in [34]. Here the drive element consists of a mono-material system. The whole drive is fabricated in one step (figure 2(g)).

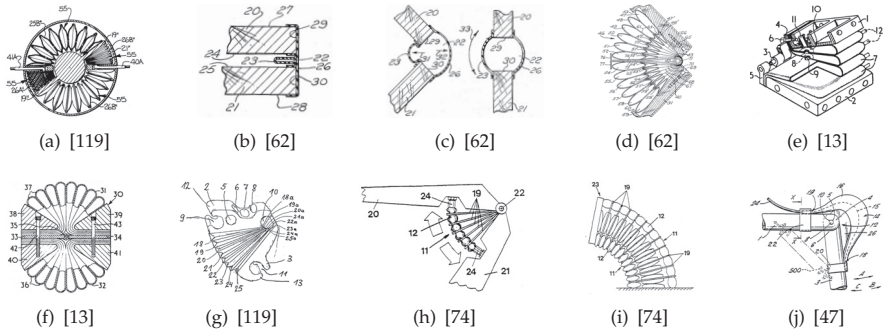

(a) [119] (b) [62] (c) [62] (d) [62] (e) [13]

(f) [13] (g) [119] (h) [74] (i) [74] (j) [47]

Figure 2. Radial Cross-Section View of Different Fluidic "Expansion" Drives

While the presented concepts are designed to operate with pressures in the range of $0 - 20\,bar$ the development in [74] is operated with pressures up to $200\,bar$. The actuator set-up allows both, linear and rotary actuation (figure 2(h), 2(i)). The focus in these works lays on heavy duty machinery but rotary drives or trunk-like structures are discussed for robotic applications as well. Detailed concepts regarding layered fiber reinforcements in the shell are introduced.

While the previous example requires complex knowledge and technology to produce an individually shaped membrane, other examples implement standard materials for flexible fluidic actuators. In [61, 81, 110] a design is proposed that uses bulky materials such as ordinary water hoses to form the actuator. Figure 2(j) shows one set-up of this FLEXATOR muscle. Subsequent developments applied the FLEXATOR technology to the fields of rehabilitation [103] and horticultural robotics [129]. The works of Prior et al. [103] introduced a unique approach that came to be known as "hybrid actuation" [117]. Here the powerful fluidic actuators are combined with precisely controllable electrical actuators in a parallel configuration.

2.1.2. Flexible fluidic "Contraction" actuators

This type of actuators generates a tensile force when pressure is applied. There is large variety of "contraction" actuators. They must be sorted into two groups. The first group includes actuators that generate a tensile force due to **"Anisotropic Membrane Stiffness"**. Daerden and Lefeber described some of those actuators in their review article [20]. These actuators increase in surface area when pressurized. The axial contraction is coupled to a radial expansion in which some of the energy is used for membrane deformation. Generally Joseph L. McKibben is said to be the inventor of the most popular design, often referred to as "McKibben Muscle". However, earlier patents describe the same design. In 1929 Dimitri Sensaud de Lavaud [22] introduced a fluidic muscle as shown in figure 3(a). This early work was later followed up by the patents of Morin [89] in 1947 and Woods [141] in 1953, where the design and characteristics of the fluidic muscle were described in detail. The actuators consist of a highly elastic inner membrane that is covered with a helically wound fiber reinforcement like a braided fiber hose (figure 3(b)). When pressurized the fiber angles change until the critical fiber angle of $\theta = 54,4^\circ$ is reached (figure 3(c)) [141].

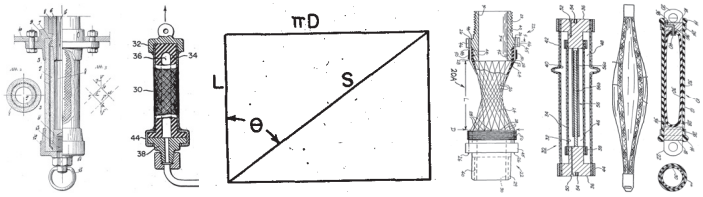

(a) [22] (b) [141] (c) geometric correlation between fiber angle θ and muscle diameter D [141] (d) [119] (e) [92] (f) [76] (g) [88]

Figure 3. Different Fluidic Muscles

In [101] Paynter describes a variation of this type of fluidic actuator. The "hyperboloid muscle" is equivalent to a prestretched fluidic muscle, which extends the range of motion (figure 3(d)). Other set-ups from Paynter are discussed in [98] and [100].

Commercially available fluidic actuators were introduced by Bridgestone Corporation, Japan, FESTO AG&Co. KG, Germany, and Shadow Robot Company, UK. Bridgestone introduced a single-acting [128] and a antagonistic [92] actuator design (figure 3(e)) but soon stopped their activities in the field. With operating pressures up to $2\,bar$ and a fatigue life of $67,000$ load cycles these actuators weren't really competitive.
Nowadays FESTO offers the biggest portfolio of fluidic muscles [29, 30]. Operating pressures are $0-8\,bar$ in connection with a fatigue life of $10,000-1\,Mio$ load cycles depending on the load case.

Lewis [76] and Monroe [88] proposed a design with only axially fiber reinforcements. Thus actuation is connected with a radial stretch of the pure rubber sections between the axial fiber strands (figure 3(f), 3(g)).

The second group of "Contraction" actuators generates the force due to **"Vectored Structural Degrees of Freedom"**. These actuator designs try to raise efficiency and to minimize the hysteresis compared to the first group of actuators. Ideally there is no strain of the membrane and almost no internal friction. When pressurized these actuators increase in volume while maintaining the same surface area. Yarlott [143] proposed a folded structure that unfolds when pressurized and thus contracts (figure 4(a))

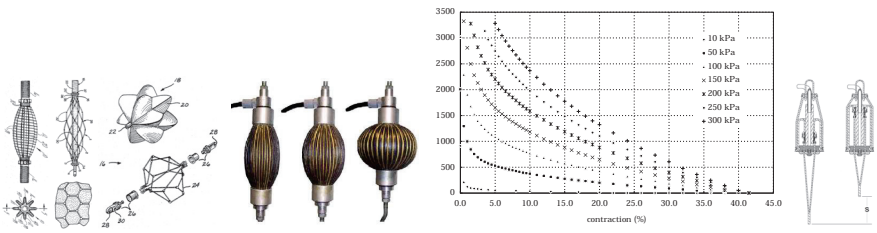

(a) [143] (b) [73] (c) [58] (d) [19] (e) [21] (f) [25]

Figure 4. Some FFAs based on "Vectored Structural Degrees of Freedom"

The work of Kukolj [73] shows an actuator with a net as the fiber reinforcement. This eliminates the friction between the fiber strands, but the friction between membrane and fiber reinforcement remains (figure 4(b)). Immega [58] enhanced this idea by implementing a stiff, folded membrane in between the fiber mesh (figure 4(c)).

A newer design known as "Pleated Pneumatic Artificial Muscles (PPAM)" was introduced by Daerden and Lefeber [19, 21]. The design is similar to the Yarlott muscle. Figure 4(d) and 4(e) show the design and the force-displacement characteristics of these artificial muscles.

Erickson [25] described a contraction actuator that can be considered an inverse rolling-lobe cylinder. This set-up has a large working range of 40-60% of the initial length (figure 4(f)).

2.1.3. Flexible fluidic "Bending" actuators

Bending actuators are generating a bending motion when pressurized, which is used to manipulate objects in an adaptive and compliant way. Staines [120] presented vacuum operated and Baer [7, 8] pressure operated conceptual solutions for this problem (figure 5(a) and 5(b)).

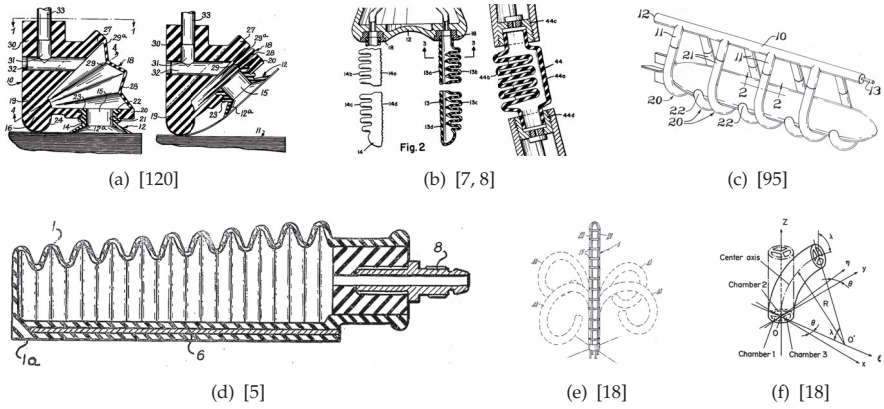

(a) [120] (b) [7, 8] (c) [95]

(d) [5] (e) [18] (f) [18]

Figure 5. Bending Actuators

The work by Orndorff and Ewing [27, 95] as well as Andorf et al. [5] introduce designs where bending occurs due to "anisotropic membrane stiffness". Craig et al. [18] point out that these types of actuators can be folded to reduce shipping volume specially for space applications. Figure 5(c)-5(e) show the different designs.

Bending actuators designed with multi-lumen hoses are represented by the work of Suzumori et al. [122–126] shown in figure 5(f). Radial reinforcements inhibit radial expansion so that the operating pressure is $1.4 - 4\,bar$.

There is a large variety of trunk-like bending actuators that create bending motion by adding structural constraints. A few examples are shown in figures 6(a)-6(c).

Monolithic bending actuators represent the last group in this section. Different research groups have been working on this topic during the last years [57, 71, 145, 146]. These actuators

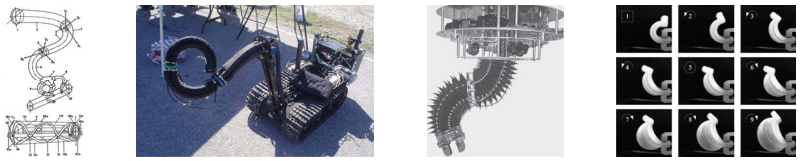

(a) [15] (b) [84] (c) [6] (d) [145]

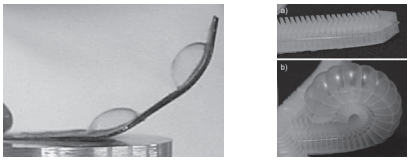

(e) [71] (f) [57]

Figure 6. Trunk-Like Bending Actuators and Monolithic Bending Actuators

are single material devices and mainly fabricated in on step. Operating pressures are mostly $< 1\,bar$. Some prototypes are shown in figure 6(d)-6(e).

2.1.4. Flexible fluidic actuators - combined motion

This group of actuators produces multiple directions of motion. Griebel et al. [38] developed a placement actuator for EEG-electrodes that conducts a linear expansion in combination with a coaxial rotation (figure 7(a)). Paynter [99, 102] on the other hand supresses the linear motion on purpose in order to design an pure rotary drive. As shown in figure 7(b) a pre-twisted membrane is straightened when pressurized and thus generates a rotary motion.

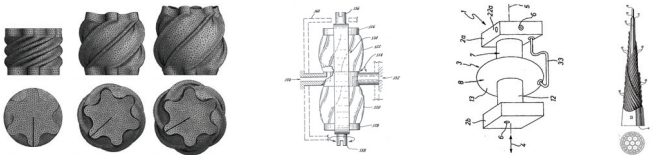

(a) [38] (b) [99] (c) [16] (d) [139]

Figure 7. Actuators with two directions of motion

Other concepts use several different cavities to create multi-motion actuators. Claus [16] presents a push-pull actuator while Wilson [139] combines expandable hoses to build a versatile robotic arm (figure 7(c) and 7(d)).

Alternative approaches are presented by Kimura and Brown. Kimura et al. [69] describe a principle that is called “whole skin locomotion”. Here an elongated toroid turns itself inside out and hence can move over surfaces or through gaps (figure 8(a)). The concept by Brown et al. [14] is referred to as “jamming of granular material”. The idea here is known from vacuum mattresses in ambulances. A flexible bag containing a granular material is shaped around an object and then evacuated. Friction, suction and mechanical interlocking connects gripper and object (figure 8(b)).

(a) Whole Skin Motion by Kimura et al. [69]

(b) Whole Skin Gripper by Brown et al. [14]

Figure 8. Actuators based on Whole Skin Effects

2.2. Flexible fluidic structural elements

Flexible fluidic structural elements complete the biomimetic approach. There are many examples of hydrostatic skeletons in nature [130].

Inflatable structures are well known in fields of crisis intervention [26] and exhibition stand construction [94]. Other applications include space structures like antennas [33, 79, 82, 132] and rovers [28, 48, 63, 72].

Most robotic designs with inflatable structures aim at space applications since they have a small shipping volume when deflated. Koren et al. [72] proposed a design for zero gravity applications and operating pressures of about 3.5 *bar* (figure 9(c)). Shoham et al. [104, 105, 118] developed a inflatable robot as shown in figures 9(a) and 9(b). They also characterized the robot regarding its stiffness at internal pressures up to 2 *bar*.

(a) inflated [118]

(b) deflated [118]

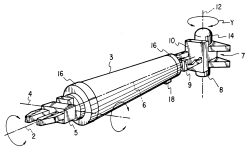

(c) [72]

(d) [106]

Figure 9. Different Robots with Inflatable Structures

The works of Sanan et al. [106], Maruyama et al. [83], and Voisemebert et al. [135] focus more on service and inspection robotics. Operating pressures are in the range of $0.4 - 0.6\,bar$. The 1-DOF arm developed by Sanan is shown in figure 9(d).

3. Flexible fluidic actuators - fabrication

3.1. FFA - Materials

As the name implies FFAs are made of flexible shell materials. This fact limits the number of relevant materials naturally. Normally laminated foils [112], vulcanized elastomers [36], coated fabrics [97], layered set-ups [1], or various combinations are used. A reasonable differentiation can be made between primary shaping processes like rubber molding and

[1] http://www.otherlab.com/

processes that use semifinished products like foils, in order to form the actuator's cavity. Both processes have their pros and cons.

3.1.1. Semifinished materials

Material selection cannot be considered without looking at the fabrication process. Of all welding technologies high-frequency (HF) welding can produce the most resilient seams [2]. However, HF-welding can only be achieved with materials that contain sufficiently strong dipoles. Thermoplastic Urethanes (TPU) have compared to PVC and PA the best material properties [144]. The latest material developments regarding composite sheet materials will be described in the following sections. The HF-welding technology is mostly used for more complex actuator technologies since the technology does not require very complicated molds.

3.1.2. Vulcanized elastomers

Vulcanized elastomers are often processed in compression molding processes. The uncured rubber monomer is put in the heated cavity of a compression mold. The press is closed and under the influence of heat and pressure the rubber is cross-linked. The variety of rubber compounds is infinite. The final material properties can be influenced by fillers, reinforcements and a large variety of chemical additives. How to achieve materials with tailored properties for flexible fluidic actuators will be presented. Compression molding requires complex molds, which limits variations in shape but provides actuators for high operating pressures.

3.2. FFA - fabrication processes

The two main processes for FFA fabrication are compression molding and HF-welding. A detailed description of both process developments is given here.

3.2.1. Compression molding

The requirements for vulcanized flexible fluidic actuators are simple:

- High pressure resistance
- High fatigue resistance
- Modular design
- Reproducible fabrication process

In order to achieve these properties the actuator shell is divided into two layers and fabricated in a two-step compression molding process. In the **first step** the inner shell is made. The inner shell (figure 10(b)) is responsible for tightness and fatigue strength of the actuator. It is vulcanized in a mold as shown in figure 10(a).

The **second step** needs some preparation. First the inner shell is covered with a braided aramid fiber sleeve, which is fixed around the rubber with a Vectran® yarn. This fiber reinforcement determines the pressure resistance of the actuator. After that the metal connectors are inserted and the mold adapters are added. Finally a thin layer of rubber is applied to the surface (figure 11(a)). The set-up is now ready for the second vulcanization

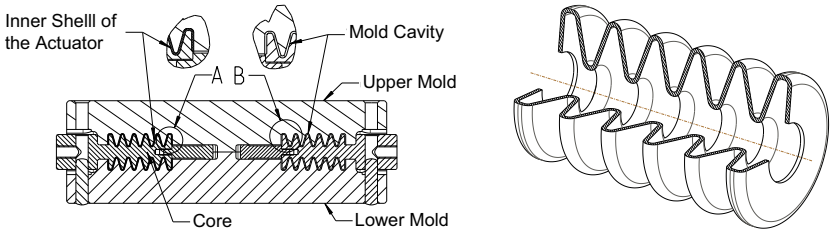

(a) Cross-section View of the first Mold

(b) Partial Section of the demolded Inner Shell

Figure 10. First Fabrication Step

step. The prepared actuator is inserted in the second mold and pressure is applied as depicted in figure 11(b). Fiber reinforcement and metal connectors are vulcanized to the inner shell.

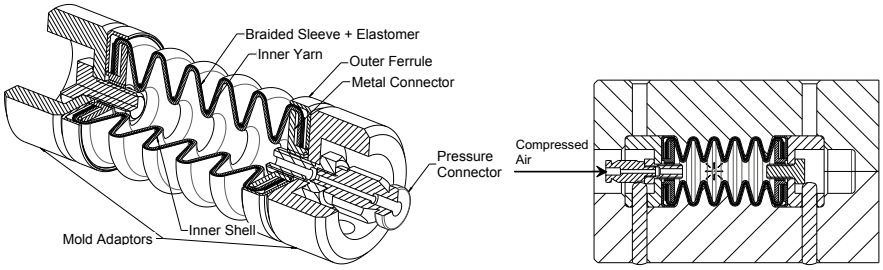

(a) Partial Section of the Actuator Prepared for the Second Fabrication Step

(b) Cross Section View of the second Mold

Figure 11. Second Fabrication Step

Operation shows that fatigue crack growth is the main failure mode of vulcanized flexible fluidic actuators. There are three main mechanisms to enhance crack growth resistance: Use of stress and strain crystallizing rubbers, use of fillers (mainly carbon black), and dispersion of pulp fibers. The first two mechanisms are implemented by the proper choice of the basis material (in our case a chloroprene rubber mixture (CR)). However, the particle morphology of carbon blacks limits their contribution to fatigue resistance [142]. Crack bridging effects can only be achieved by dispersing micro fibers in the basis elastomer. Aramid fiber pulps are well-suited for this purpose [3, 70, 131]. With a specific surface are of $5 - 15 \frac{m^2}{g}$ and a minimal fiber diameter of $10\,\mu m$ they can enhance the overall material properties significantly (figure 14).

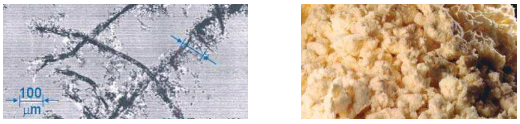

(a) Single Pulp Fiber

(b) Aramid Fiber Pulp

Figure 12. Morphology of Fiber Pulps

In order to determine the best concentration masterbatches with 0,5%, 1%, 2%, and 5%-mass have been tested according to DIN 53 504. Figure 13(a) shows how the pulp fibers get oriented in flow direction. Hence the samples with parallel and orthogonal pulp fiber orientation have been tested. The orientation has a significant influence on the force-displacement characteristics. The figures 13(c)-13(d) shows crack surfaces with different fiber orientations.

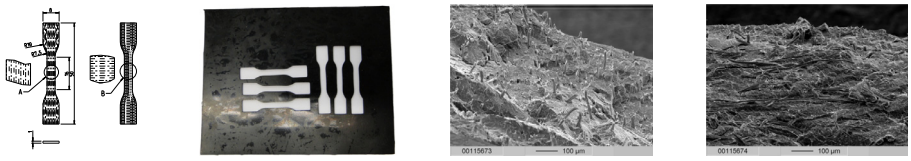

(a) Sample Geometry and Pulp Fiber Orientation

(b) Sample Plate

(c) Pulp Fiber Orientation Parallel to Crack Surface

(d) Pulp Fiber Orientation Orthogonal to Crack Surface

Figure 13. Material Characterization

Generally the goal is to define the maximum fiber concentration that does not lower the tensile strength significantly. The results show that a concentration of 1%-mass leads to the best material properties. The force-displacement plots show a clear influence of the fiber orientation, but in parallel configuration there is no significant difference compared to the pure rubber material (figure 14).

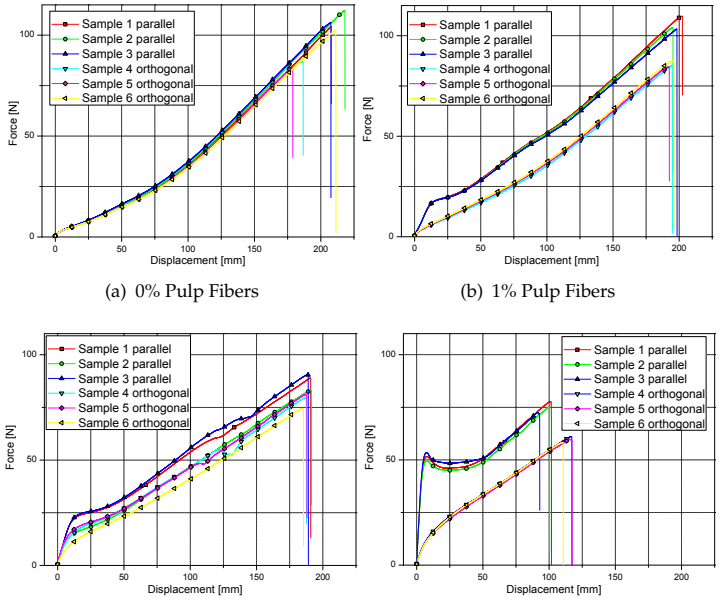

(a) 0% Pulp Fibers

(b) 1% Pulp Fibers

(c) 2% Pulp Fibers

(d) 5% Pulp Fibers

Figure 14. Force-Displacement Plots for different Pulp Fiber Concentrations

3.2.2. High frequency welding

Commercially available fiber reinforced TPU foils show several drawbacks, such as low tensile strength, delamination between fibers and TPU-matrix, and axial fiber porosity. The general requirements for HF-welded FFAs are:

- A maximum thickness of 700 μm
- A tensile strength between 30 and 100 $\frac{N}{mm^2}$
- A modulus of 100 to 150 $\frac{N}{mm^2}$
- Gas-tight including no axial fiber porosity
- Odourless
- Processable with HF technology

Two material systems meet these requirements. **PEEK-monofilament reinforced TPU films** are composite sheets with two layers of monofilament PEEK-mesh between three layers of TPU-films. The overall material properties are: tensile strength 33 $\frac{N}{mm^2}$, Young's modulus of 168 $\frac{N}{mm^2}$, specific weight 269 $\frac{g}{m^2}$, thickness 450 μm.

Aramid-fiber reinforced TPU films are processed slightly different. Since the aramid fibers are spun to a yarn and are not available as monofilament material with sufficient strength, the yarn must be sealed prior to the laminating process. This is done by applying a TPU solution on the aramid fabric. After the evaporation of the solvent all yarn surfaces are covered with a thin layer of TPU. The pretreated aramid fabric is then laminated between two layers of TPU film. The resulting material properties are: thickness 580 μm, specific weight 365 $\frac{g}{m^2}$, tensile strength 60 $\frac{N}{mm^2}$.

A schematic view of the general production process is illustrated in figure 15. The inter-chamber connections of the pre-cut foil pieces are welded first. These pre-assembled pieces are then welded together around the outer contour in as many layers as desired. This second step closes the actual actuator chamber.

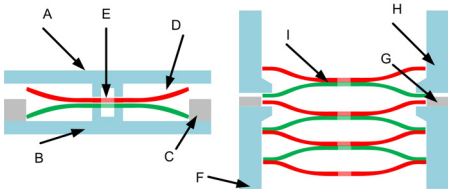

Figure 15. (A) upper welding electrode, (B) lower welding electrode, (C) centering coil, (D) two foil pieces, (E) hole for air passage, (F) lower welding electrode with undercut, (G) centering coil, (H) upper welding electrode with undercut, (I) foil segments from first step

3.3. FFA - evaluation

All dynamic testing was accomplished on a fatigue test rig consisting of a pressure-tight container, in which the actuators are mounted. The pressure in the container is monitored which allows detection of leaks in the actuators.

3.3.1. Vulcanized actuators

The relationship between fatigue resistance, operating pressure, and material combination is shown in figure 16. The choice of the base rubber compound influences the fatigue resistance significantly. The best fatigue resistance can be achieved with CR-rubber containing 1%-mass of aramid pulp fibers. At 6 *bar* the actuator withstands over 1,200,000 load cycles. In order to keep testing simple all fatigue evaluation was carried out with actuators 18 *mm* in diameter. All actuators failed due to fatigue cracks in the inner rubber shell. This results in excellent fail-safe characteristics, since the actuator never bursts and can be changed without any danger to the whole system.

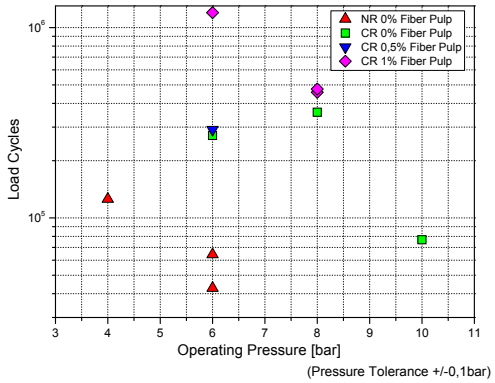

Figure 16. Fatigue Resistance of 18 *mm*-Actuators

3.3.2. HF-welded actuators

To evaluate the influence of the various production parameters during HF-welding on lifespan, several endurance tests were performed. In these tests, one parameter is varied and all others kept constant. Each experiment was performed with ten actuators. This was necessary because the deviation in lifespan was about 30% of the average lifespan. The influence of the following parameters on the lifespan has been determined:

- **Determination of the geometry of the welding tool:** In this test it was determined how the geometry of the welding tool influences the lifespan of the actuators. The first tool set-up consists of two electrodes (ground and high frequency) with the same geometry and mass. The second tool set-up consists of one electrode (high frequency) with the shape of the weld seam. The other electrode (ground electrode) is a flat plate.
- **Identification of the most durable seam thickness:** The seam thickness was varied between 95% and 15% of the total strength of the two films in order to determine which weld strength achieved the longest lifespan. In this experiment it was also determined how thick or thin a seam can be produced.
- **Variation of the welding force:** It was determined how the welding force, pressing the two electrodes together, affects the lifespan. This parameter indirectly sets the temperature at which the seam is formed.

- **Varying the time of the load cycle:** In addition to previous experiments where the load cycle time was six seconds (3 *s* pressure / 3 *s* no pressure) the cycle times were varied at 2, 4, 6, 10, and 20 seconds.
- **Evaluate the best pressure rise time:** In this experiment the actuators were filled via a restrictor. So the time to fill is adjustable. These different times were 40, 125 and 250 *ms*. A shorter time than 40 *ms* between the electrical signal to the switching valve and the reach of 95% of the desired pressure was technically not possible.
- **Evaluate the best release time:** Analogous to the determination of the pressure rise time, the pressure reduction period was varied. The restrictors were used with the same settings as the pressure rise test.
- **Limitation of the expansion:** This test was necessary to evaluate the effect on durability when the maximum deformation is limited. The expansion is limited to 100, 66, 50, and 33%.

It has been found that the lifespan increases when the deformation speed is low. When the pressure rise time is six times higher (40 $\rightarrow$ 250ms), the lifespan increases by a factor of 2.5. The pressure release time influences the lifespan similarly. The limitation of the maximum expansion to 50% of the nominal stroke increases the lifespan by a factor of 4. The use of two electrodes with the same mass and same shape also creates an increase by a factor of 2. The production of a seam with a higher initial welding force also has a positive effect on the lifespan of the actuators. This increase is only about 10%. The optimal seam thickness varies depending on the structure of the material used. The increases on the lifespan which can be achieved with this optimization are by a factor of two. Weld seams with a thickness less than 20% or greater than 80% of the nominal thickness of the two films are not useful. The variation of the load cycle time shows that the actuators fail very quickly at an operating frequency of 6 seconds. For longer load cycles, the composite material has more time to relax and reduce internal stresses. With shorter cycle times the internal stresses caused by the previous load cycle are not yet dissipated and a kind of solidification occurs.

Endurance tests of actuators with different film materials were conducted in order to compare the film properties.

- **Determination of the lifetime curve:** These tests were conducted with ten actuators for each pressure step. This pressure was applied cyclically to determine the durability of the actuator as a function of pressure. Pressure values of 3, 4, 6 and 8 *bar* were used. All tests were carried out using a commercial film material.
- **Continuous operation of the actuators of PEEK reinforced TPU film:** With ten actuators made of this material an endurance test at six bar and a cycle time of 6 seconds was performed. In this endurance test, the results of some of the previous test runs were considered. The thickness and the initial load were adjusted. The other parameters like pressure rise/release time, expansion ratio, and welding tools have not been altered to ensure the comparability of results.
- **Continuous operation of the actuators of aramid reinforced TPU film:** The parameters of this endurance test were identical to those of PEEK actuators.

Determining the lifespan trajectory has shown that the operating pressure has a big effect on the durability. If the average lifetime at 6 *bar* of about 500 cycles is set to one, the actuators

achieve at 8 *bar* only the value of 0.2. At a pressure of 4 *bar* they reach a 8 and at 3 *bar* they reach a value of 66. In comparison, the average lifetime of PEEK actuators at 6 *bar* is around 112 and 205 for the aramid-reinforced actuators. The failure mode mostly was breaking of the weld between the tube and the TPU.

4. Series of flexible fluidic actuators

Over the years, a large variety of flexible fluidic actuators have been developed. The following sections give an overview of the most recent models either fabricated by compression molding or HF-welding.

4.1. Vulcanized Actuators

All vulcanized actuators are fabricated using the process described in chapter 3. This process represents a scalable and reproducible fabrication process resulting in the following actuator geometries. Figure 17 gives an overview over all rubberbased FFAs. Each section includes the general properties and the actuator characteristics. The standard operating pressure is $0 - 10\,bar$ for all vulcanized FFAs.

Figure 17. Series of Vulcanized FFAs: (from left to right) 36mm, 18mm, 11mm, and single chamber FFA

4.2. HF-welded actuators

HF-welded actuators and the corresponding joint modules have been called GPA (Gelenkmodul fuer Pneumatische Aktoren). GPAs have already a fairly long and successful history as can be seen from the different generations shown in figure 18. The emphasis of continuing developments is improving the lifespan of actuators, the welding process, the maintainability, and some economic aspects.

GPA Type	Torque [Nm] (min. - middle - max.) at 4 bar	Range of Motion [°] at 4 bar	Dimensions [mm]	Weight [kg]	number of parts to be machined
T1-14T	3 - 10 - 14.5	±83	85x75x70	0.25	16
T2-13RVD	2.1 - 9.9 - 17.6	±85	110x95x80	0.26	6
T3-12RVD	1.7 - 7.1 - 13	±116	103x80x69	0.18	10

Table 1. Properties of different GPA versions

In table 1, the actuator designators define the number of chambers and the material. The range of motion depends on the applied pressure because the antagonistic actuator needs to

∅ 11mm Actuator:

- Effective Diameter of 11 *mm*
- 5 Pleats
- Range of Motion 90°
- Symmetric Shape

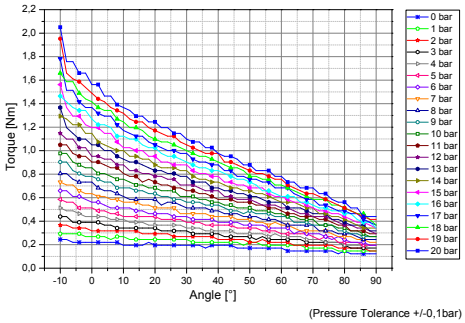

(Pressure Tolerance +/-0,1bar)

∅ 18mm Actuator:

- Effective Diameter of 18 *mm*
- 5 Pleats
- Range of Motion 90°
- Symmetric Shape
- Burst Pressure $>$ 40 *bar*

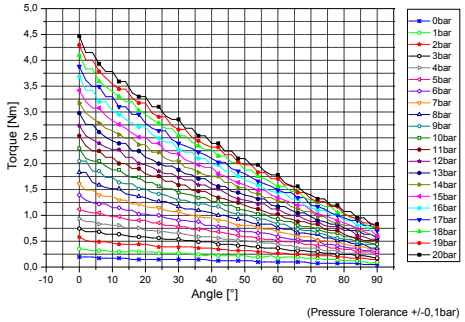

(Pressure Tolerance +/-0,1bar)

∅ 36mm Actuator:

- Effective Diameter of 36 *mm*
- 6 Pleats
- Range of Motion $\pm 90°$
- Asymmetric Shape

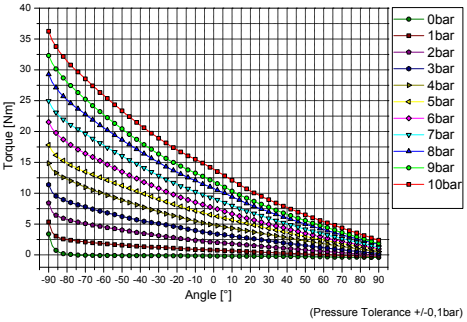

(Pressure Tolerance +/-0,1bar)

Single Chamber Actuator:

- Effective Diameter of 40 *mm*
- 1 Pleat
- Range of Motion $\pm 12°$ or 19*mm* Linear Motion
- Symmetric Shape

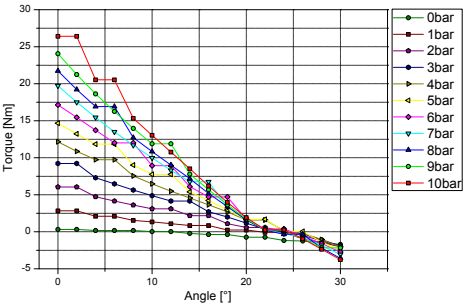

(Pressure Tolerance +/-0,1bar)

be compressed and thus the range of motion depends on the applied torque. Except for the extreme angular ranges, the torque over angle is fairly linear. Figure 19 shows the torque-angle plot for different pressure values.

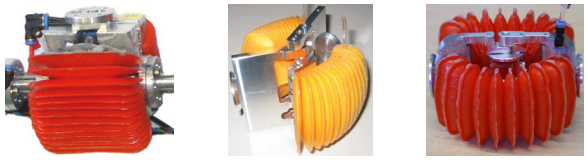

(a) GPA 1 (b) GPA 2 (c) GPA 3

Figure 18. The three GPA generations

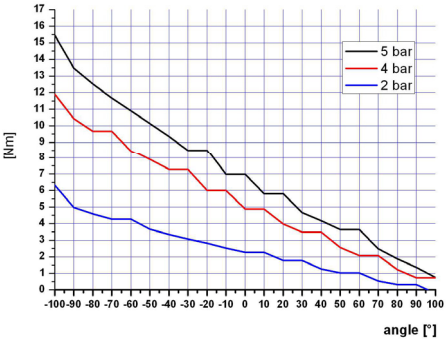

Figure 19. Torque-Angle Plot for GPA-3 module with a 10 chamber actuator

Of course table 1 does not reflect all the important parameters. For example, the lifespan of actuators has grown dramatically from a view thousand up to more than 350,000 stress cycles (full range motion with 4 *bar* forth and back in 3.6 *s*) for GPA3.2 joint modules. Lifespan depends very much on the maximum applied pressure and the valves to be used. The value of 4 *bar* is a good compromise between maximal torque and lifespan. Most GPA types may be operated using higher pressure (up to 6 *bar*), but the lifespan of actuators will decrease dramatically at this pressure. In many cases repair welding is possible.

5. Designing with flexible fluidic actuators

5.1. Design principles

Using flexible fluidic actuators as drives makes the designing process comparatively easy. Since the compressive force of the actuator is directly used to generate torque, no additional transmission elements are necessary. However, the flexible properties of the actuators require guiding components along the the actuators track of motion. If those guiding elements are not included, the actuator will work, but will eventually have decreased range of motion and less torque. The guiding elements for vulcanized actuators are metal connectors at the end of the actuator and additional metal brackets in the midsection of the actuator. HF-welded actuators mainly use additional lugs around the chambers which are included in the seams or the end areas of the actuators. These lugs are then clamped in the structure of the corresponding joint. Position and type of the guiding element are additional parameters to determine the overall characteristics of the flexible fluidic drive.

5.2. Operating flexible fluidic actuators

The requirements to operate FFAs are pressure supply, control members, and sensory infrastructure. Depending on the complexity of control that is desired, control members and sensors can include valves, position sensors, pressure sensors, and micro controllers. A detailed overview for highly integrated FFAs is given in [1]. Using hydraulics for mobile applications instead of pneumatics can help to avoid bulky pressure supplies.

5.3. Structural modeling of flexible fluidic actuators

Structural and material nonlinearities as well as large strains make it very hard to predict the behavior and characteristics of flexible fluidic actuators. Thus implementing a structural model of FFAs is a challenging task. The FEM-model was developed with ANSYS in order to provide a design tool for FFAs. The configuration of the model is illustrated in figure 20. The different layers of the actuator shell are modeled using different elements. The inner and outer rubber shell is modeled with 941,902 SOLID285-elements using a hyperelastic material model according to YEOH [2]. The fiber reinforcement is represented by 13,428 SHELL181-elements which are connected to REINF265-elements respectively [3]. The structural integrity of the corresponding joint is modeled using 1,502 MPC184-Link/Beam-elements. The metal brackets are implemented using 14.042 SOLID185-elements [4]. Including the contact elements, the model consists of 1,235,804 elements.

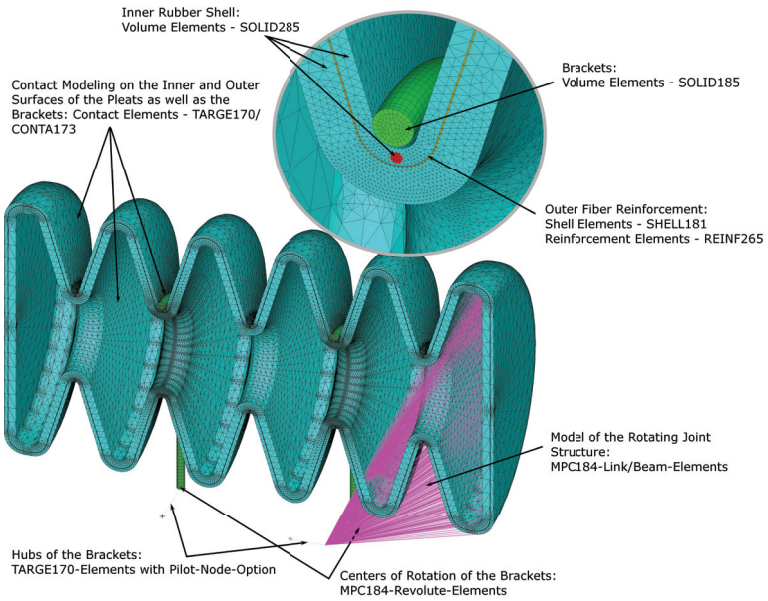

Figure 20. Set-up of the FEM-Model for a Flexible Fluidic Actuator

[2] $C_{10} = 0.477330421717; C_{20} = -0.148261658100; C_{30} = 0.225732915194$
[3] Young's Modulus $E_{\parallel} = 124 \frac{kN}{mm^2}$; $E_{\perp} = 8 \frac{kN}{mm^2}$; Poisson's Ratio $\nu = 0.32$
[4] Young's Modulus $E = 210 \frac{kN}{mm^2}$; Poisson's Ratio $\nu = 0.32$

In order to compare the structural model with the behavior of the real actuator at first a strain analysis is conducted. Figure 21(a) compares the strain behavior of the model and the real actuator for joint motions of $0° - 90°$. The comparison shows good compliance of model and actuator.

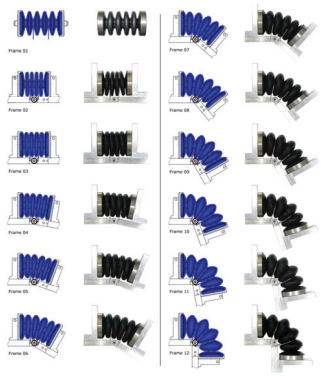

(a) Strain Analysis of a Flexible Fluidic Actuator ($\varnothing 18mm$), FEM-Model vs. Real Actuator

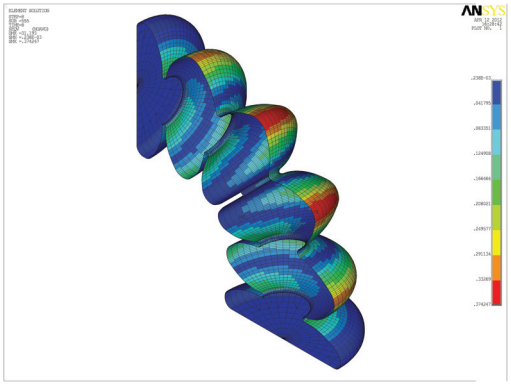

(b) Stress Analysis of the Fiber Reinforcement of a Flexible Fluidic Actuator ($\varnothing 18\,mm$)

Figure 21. Structural Analysis of the Actuator Model

The stress analysis of the fiber reinforcement in the actuator shell is shown in figure 21(b). The regions of high stress correspond with the areas where fatigue failure occurs.

6. Modeling and control of flexible fluidic actuators

From the control point of view, FFAs represent a complex dynamic system of high nonlinearity. In contrast to conventional fluidic actuators, FFAs posess some important properties, which are essential with respect to modeling and control problems:

- as a consequence of using viscoelastic materials for the chamber manufacturing, actuator torque and volume characteristics are complex non-linear functions not of pressure only, but also of angular displacements
- there are no "classical" sealing elements with static friction and stick-slip effects, but the viscose friction and damping effects can play an important part
- hysteresis effects by torque generating are indicated

Due to restricted volume of this section, the modeling and parameter identification approaches as well as different control concepts will be presented briefly. More details can be found in the related references.

6.1. Modeling

Generally, the model of FFA as a torque source consists of a model of actuator mechanics and pressure dynamic model. The modeling process includes the experimental investigation of the basic actuator characteristics with following data fitting.

6.1.1. Mechanical model

Using FFAs, a compliant robotic joint of rotary type can be realized either as an antagonistic set up with two working chambers (Fig. 22a) or as a unit with one working chamber and a retraction spring (Fig. 22a). Fig. 22 shows mechanical schematics of the both joint types.

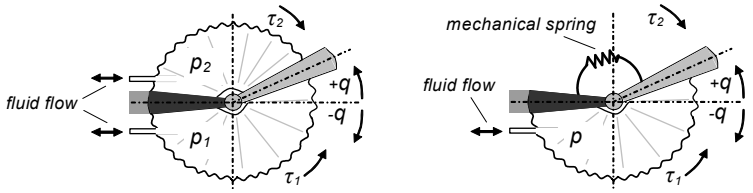

(a) with two antagonistic assembled flexible chambers

(b) with one flexible chamber and a retraction spring

Figure 22. Working principle of a fluidic actuated rotary robotic joint

As shown in previous sections by means of experimental investigations (static load tests), the static torque characteristics of the FFA are in general nonlinear functions not only of the operating pressure p only, but also of the working angle q. This is a basic feature of FFAs, in contrast to conventional fluidic actuators like pneumatic and/or hydraulic cylinders or vane actuators and the source of inherent compliancy of FFAs. Taking into account this basic feature, the total torque for the compliant robotic joint with antagonistic set-up can be determined as

$$\tau\left(q,\dot{q},p_1,p_2\right)=\tau_1\left(q,p_1\right)-\tau_2\left(q,p_2\right)-\tau_{loss}\left(q,\dot{q},p_1,p_2\right) \tag{1}$$

or as

$$\tau\left(q,\dot{q},p\right)=\tau_1\left(q,p\right)-\tau_2\left(q\right)-\tau_{loss}\left(q,\dot{q},p\right) \tag{2}$$

for the joint with one flexible chamber and a retraction spring. Here τ_1 and τ_2 represent static actuator torques acting in positive and negative directions respectively, τ_{loss} represents the torque losses like viscous friction (damping) and can include also tourque/angle hysteresis. These effects are typical for soft fluidic actuators (including linear pneumatic muscles) and are an inevitable consequence of using viscoelastic materials in the chamber. The results of experimental investigations of basic characteristics and dynamic modelling of compliant fluidic robotic joint operated by gaseous as well as liquid working media, was reported in [86, 87] and summarized in [85], whereby the torque losses τ_{loss} was measured in first approximation in the experiments at constant velocities. The hysteresis was measured, performing the torque measurements in opposite angle directions. The torque characteristic $\tau_i\left(q,p_i\right)$ of an individual chamber i, experimentally determined during static load tests, can be analytically described by means of a third-order polynomial with angle q as independent variable, as

$$\tau_i\left(q,p_i\right)=\kappa_3\left(p_i\right)\cdot q^3+\kappa_2\left(p_i\right)\cdot q^2+\kappa_1\left(p_i\right)\cdot q+\kappa_0\left(p_i\right), \tag{3}$$

where the polynomial coefficients $\kappa_3...\kappa_0$ are functions of pressure in the chamber. For control purposes, the torque characteristic 3 can be approximated well by using the polynomial fit with six constant polynomial coefficients $k_5...k_0$ [86]:

$$\tau_i\left(q,p_i\right)=k_5\cdot q^3+k_4\cdot q^3+\left(k_3\cdot p_i+k_2\right)\cdot+k_1\cdot p_i+k_0, \tag{4}$$

The mean relative error of this simplest satisfactory approximation is < 9% (see [85] for more details).
Assuming the identity of both actuator chambers, the torque τ_2 of the antagonist chamber in (1) can be obtained by mapping the torque τ_1 of the agonist symmetrically with respect to the ordinate as

$$\tau_2 (p_2, q) = \tau_1 (p_1, -q) \ \ for \ p_1 = p_2. \tag{5}$$

The second term in (2) when using a mechanical spring with a linear characteristic can be determined as $\tau_2 (q) = c_S q$, where c_S is a spring constant. Despite obvious uncertainties, especially in FFA torque losses and fluctuations in model parameters due to behaviour of viscoelastic material, model (1) - (5) can be useful for approximate description of FFA torque characteristics.

6.1.2. Pressure dynamic model

In the case of pneumatics (i.e. for FFA, operated with a gas/air), the pressure dynamics in an actuator chamber i can be described by

$$\dot{p}_i = \frac{\chi}{V_i} \left(RT\dot{m}_i - p_i \dot{V}_i \right), \tag{6}$$

where R is the universal gas constant, T is the air temperature, V_i is the chamber volume, the mass flow rate $\dot{m}_i$ defines the amount of air, passing through a valve into or out of the chamber in a time unit. It is assumed that the heat transfers at chamber's charging and discharging are the same polytropic processes, characterized by the polytropic coefficient χ. This topic is discussed in more detail in [85]. The volume characteristic of an elastic chamber is a nonlinear function of current displacement angle q and pressure p_i. Based on the experimental data it can be approximated as

$$\dot{V}_i (q, p_i) = \nu_1 (p_i) q^2 + \nu_2 (p_i) q + \nu_3 (p_i) \tag{7}$$

where values of polynomial coefficients ν_1, ν_2, ν_2 are functions of pressure [64]. Similar to the torque characteristic, the volume characteristic of the FFA-based soft robotic with antagonistic set up is assumed to be symmetrical with respect to the joint angle:

$$\dot{V}_1 (q, p_1) = \dot{V}_2 (-q, p_2) \ \text{ for } p_1 = p_2. \tag{8}$$

The air mass flow rate $\dot{m}_i$ through the valve can be modeled by the standardized expression for air flow through an orifice (ISO 6385), whereby the orifice area varies with control input [85]. To provide a more exact model for servovalves, taking into consideration also the hard nonlinearities as the dead zones, an experimental procedure for obtaining of the real relationship

$$\dot{m}_i = f_m (u, p_{us}, p_{ds}) \tag{9}$$

between the air flow, the input voltage u to the valve, as well as the up- and downstream pressures (i.e. p_{us} and p_{ds} respectively) were applied [64, 137]. To achieve a model that describes the complete behavior of valves, both charging and discharging processes were explored for constant chamber value, inflow and exhaust flow maps were

calculated and then combined. In case of chamber charging, the upstream pressure is equivalent to the supply pressure (i.e. $p_{us} = p_s$), while the downstream pressure is equal

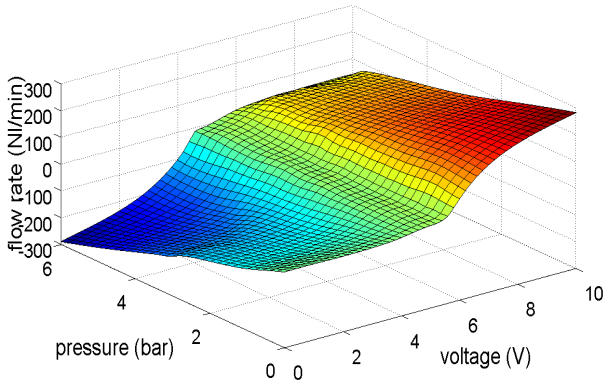

Figure 23. Experimentally determined flow map for the servo-valve Festo MPYE-5-1/8LF-010-B.

to the chamber pressure ($p_{ds} = p_i$). In case of chamber discharging, the upstream pressure is equivalent to chamber pressure ($p_{us} = p_i$) and the downstream pressure equals to atmospheric pressure ($p_{ds} = p_a$). Assuming that p_s and p_a are constant, expression 9 can be rewritten as

$$\dot{m}_i = f_m\left(u, p_i\right) \tag{10}$$

Fig. 23 shows an example of the experimentally determined characteristic of a servo valve.

6.2. Embedded control approach

In section 4 different kinds of FFAs and joint modules have been described. These actuators and joint modules were not developed with only one special application in mind. The main advantages of FFAs are their compactness and high torque to weight ratio as well as their inherent compliance. Thus it is wise to have a broad palette of solutions w.r.t. control of joint modules. Constituents for requirements for a joint module toolbox might include

- economic solutions,
- degree of compactness,
- quality of control and maximal joint rate, and
- modularity

to name the most important ones. Of course many other aspects like environmental ones may be considered (e.g. under water operation). Economic aspects might include overall costs, especially relative costs of joint module and components needed for control. Other aspects might address the lifespan of actuators, which is a compromise between maximum pressure to be applied and lifespan of actuator, type of actuator etc. Economic aspects may also include energy, consumption of compressed media, but also system integration aspects will play a role. The degree of compactness is dependent on the degree of integration of control components like sensors, valves and control logic. It also depends on the amount of tubing and cables needed for operation. High quality of control most often relies on stability, precision of position, tracking accuracy, torque precision, degree of overshooting, and bandwidth of control. In general, the more ambitious the requirements for control are, the

higher will be the costs especially for the valves. The higher the required bandwidth of control, the larger the valves will be. The pure size of the valves are in contradiction to compactness and weight requirements [**?**]. To some degree this also holds for sensor system and control and communication logic. High integration will enhance modularity when viewed from a higher standpoint where a joint module is one of many more other parts of a plant. With a closer view of a joint module, high integration will in general restrict the range of control components which can be used. Modularity should not only mean mechanical modularity but also different options for supply of compressed air, for electrical power supply, and for communication and system integration. A range of actuator solutions arranged by the degree of mechatronic integration is shown in Figure 24.

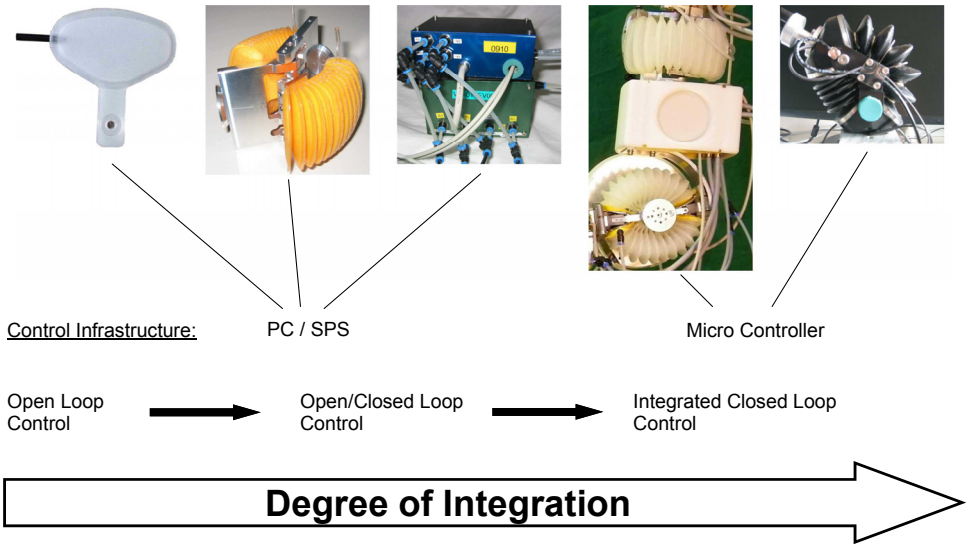

Figure 24. Different Degrees of Integration of the Control Components and Drive Systems

In this section our approach and solutions for embedded control as well as the achieved results will be described in more detail. The realization is around a 16-bit microcontroller (MC), a PIC24HJ128GP506 of Microchip with 40 MIPS performance and a broad variety of peripherals including communication via CAN. A miniature controller board CBR2 has been developed, and is able to control up to two joint modules reading joint values via 2 SPI-interfaces, pressure values via I2C or analog channels and control of switching valves by 8 output compare modules configured for PWM-mode. Control system integration is handled by an upper level control system on a PC running a user interface and coordinating different joint modules. Communication between MC and PC may be via RS232 and/or via CAN. The MC understands a simple 2-byte-command set with instructions for position set point, position ramp, torque command, pressure control, gravity compensation, parameter setting and for definition for periodical delivery of local information (to be specified by the PC) in a programmable rate with periods down to 21ms via CAN for one joint and 45 ms for 6 joints. General programming considerations relate efficiency of control calculation programming and means for utilizing parallelism. As no operating system kernel is used, mainly interrupt routines and the chipset inherent and in parallel running subunits are used. This works

very well for analog input of pressure signals and for CAN-message communication. Up to a certain level of analog signal information blocks as well as CAN message blocks are handled by DMA transfer autonomously without putting load on the CPU kernel. Message processing is implemented by a main loop, and the sampling task is a high priority interrupt task. The microcontroller does not offer floating point operations at the instruction level. Table 2 gives a hint of the relative efficiency programming int-, long int- and floating point operations [5]. Therefore mainly int16 was needed (e.g. to get more decimal places) long int (=int32) operations including shifting were used. This also means, that calculations for control algorithms were kept relatively simple. Trigonometric functions are implemented via tables:

Operator	+	-	$*$	$\div$	»const.	<
int	2	2	2	20	1	13
long int	6	6	11	469	6	16
float	124	148	118	380	-	77
double	140	152	113	383	-	77

Table 2. Instruction cycles for different operators and operands

For control of pneumatic actuators by an MC we use 2/2-way solenoid switching valves, (2 valves per actuator) one for inflation and one for deflation. Thus four valves per joint are needed, although for some cases one actuator might be replaced by a passive spring. This case will not be considered here. Presuming that a valve is sufficiently tight for higher pressure values, the maximum torque of the joint is not dependent on the maximal flow of the valves. Thus relatively small valves may be used if no special requirements for maximum speed/control bandwidth are given. The most compact and light weight valves are spider type valves. Additionally we mainly use modified double arranged switching valves of mass flow of $Q_n = 16$ SLPM (standard liters per minute) for EV08-type valves and 22 SLPM for EV09-type valves. Switching time is about $2\,ms$. These valves are light and compact enough to be integrable as demonstrated in Figure 24. For higher control bandwidth, higher mass flow is necessary. One may either operate two or more valves in parallel as one logical valve or use other models with higher mass flow. For torque and for position control pressure control is used. To measure pressure we use amplified pressure sensors with analog or I2C interface, 1ms response time and 10 bit resolution for a pressure range up to 7 bar. Using the MC's PWM features one can control mass flow by manipulating the length of the duty cycle. In our case a duty cycle has a maximum length of $7\,ms$, the sampling time of our control loop (142 Hz), which amounts to a PWM value of 1094. Unfortunately mass flow is also dependent on the type and the exemplar of valve, power supply voltage, and pressure difference. This means a model for each valve is needed. One must distinguish between the valve responsible for inflation and the one for deflation. In the first case, the pressure difference is given by the constant supply pressure and the actual pressure in the actuator. In the second case the pressure difference is between internal pressure and the $0\,bar$ environment. In Figure 25 the measured flow model is shown for inflating and deflating direction.

If one transforms flow values to the percentage scale, one gets a fairly linear relation, except for PWM values where inflation/deflation starts as can be seen in Figure 25(d). By means of interpolation using two characteristic curves for valve modelling, the MC can approximately set the percentage of mass flow given the actual pressure in the actuator. For control of mass flow a third characteristic curve will be needed.

[5] C30-Compiler, no optimization

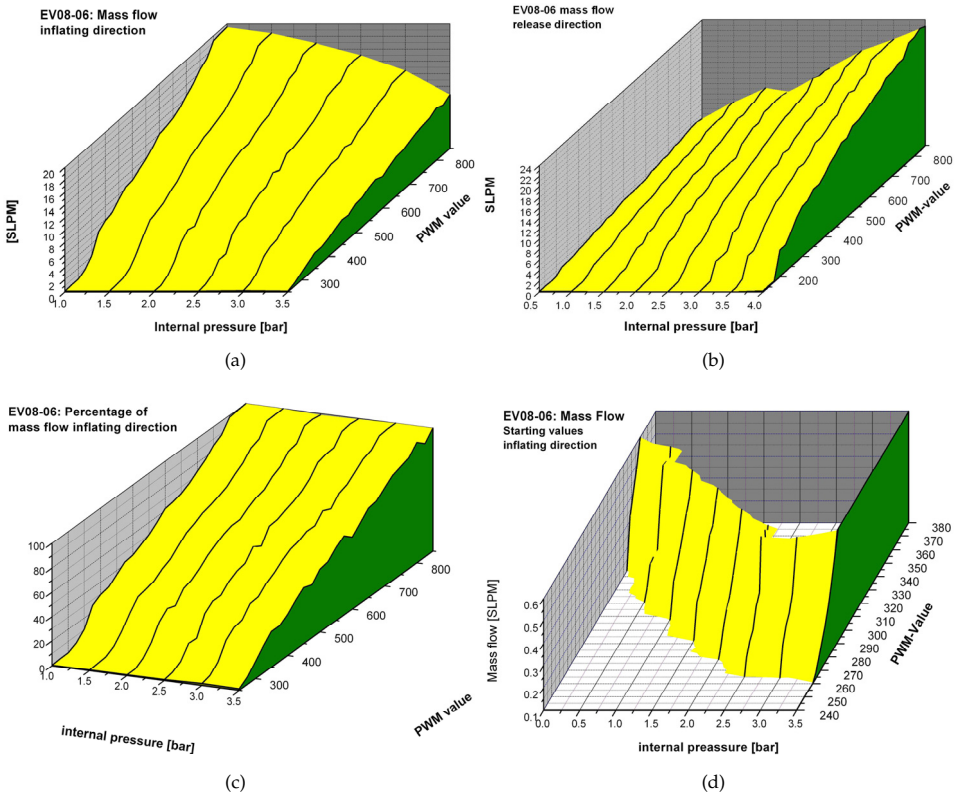

Figure 25. Flow Charcteristics of an EV08-Switching Valve

Based on such models, pressure control according to the scheme shown in Figure 27(a) give results shown in Figures 26(a) and 26(b).

In Figure 27(a), q denotes angular position, q_s position set point, p_i denotes internal pressure of actuator 1 and 2 respectively. Position control may be designed as a cascade on the base of pressure control and thus can build up (virtual) torque level using the linearized torque characteristic. Position control may also be implemented without pressure control (avoiding pressure sensors). Such schemes rely heavily upon the antagonistic actuator and use it as a kind of brake. Generally such schemes show decreased performance, may clip the angular range, have less stability and in many cases consume more compressed air. Figures 26(c) and 26(d) show position control results for different loads and different valve arrangements. The controller scheme is shown in figure 27(b).
It is difficult to achieve higher accuracy than for example $0.5 - 1^{\circ}$. This is due to the accuracy of valve control and to some degree of stochastic behavior in the flow starting part of the valves as well as limited position sensor accuracy giving poor velocity information. 14-bit sensors [AS5048 from AMS] are on the market and MC-technology is developing at a fast pace, so that there is a good chance tuning and quality of embedded control will soon improve.

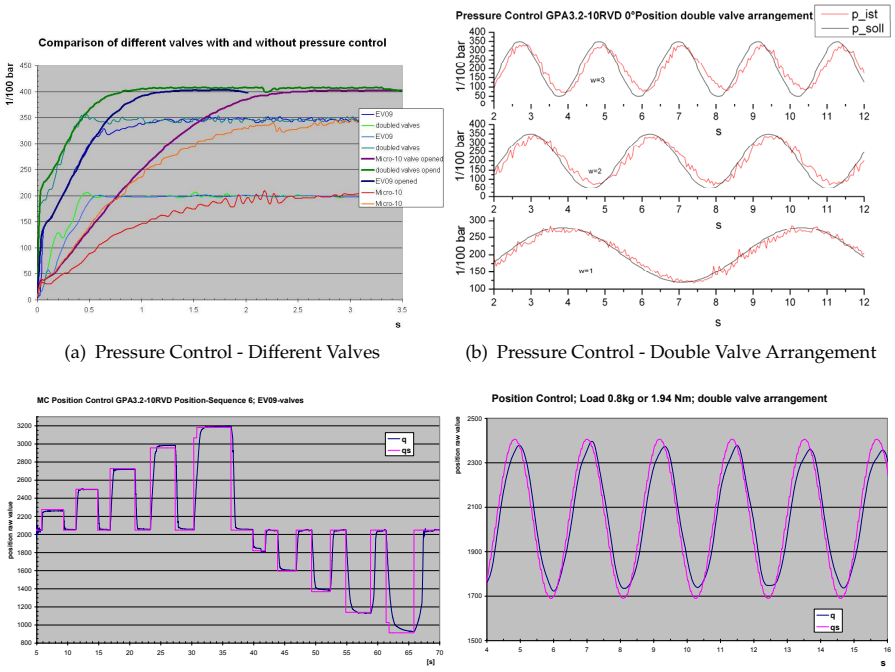

(a) Pressure Control - Different Valves

(b) Pressure Control - Double Valve Arrangement

(c) Position Control - Single EV09-Valve

(d) Position Control - Double EV09-Valve

Figure 26. Results of Embedded Control using Switching Valves

6.3. Advanced control concepts

Implementation of advanced control concepts requires the use of a high-performance PC-based controller. The control concept has a cascade structure and is applied for both (pneumatic and hydraulic) FFA realizations [85]. Control algorithms for pressure, position and interaction control for single FFA as well as for compliant robotic arms, using different valve types, were developed and tested.

6.3.1. Pressure control

Fast and precise pressure control in the inner loop of the cascade control scheme is necessary for effective control of FFAs. To decouple the pressure subsystem from the mechanical subsystem, a control law was derived using the feedback linearization approach, which was modified with regards to specific traits of soft actuators [85]. In order to compensate non-linearities of FFAs pressure dynamics, model (6) - (7) of actuator chamber volume is used in control law as feedback and for the determined flow rate the control voltage is obtained by inverting of experimental flow map (figure 10). The effectiveness of designed pressure controller has been confirmed through several experiments (step response), in pneumatic case both for PWM-controlled on-off valves [86] as well as for different types of servo valves [64, 137].

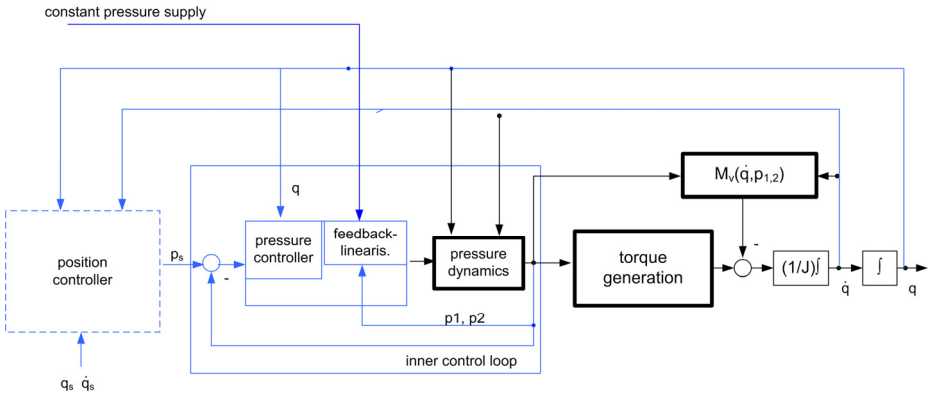

(a) Pressure Control Scheme

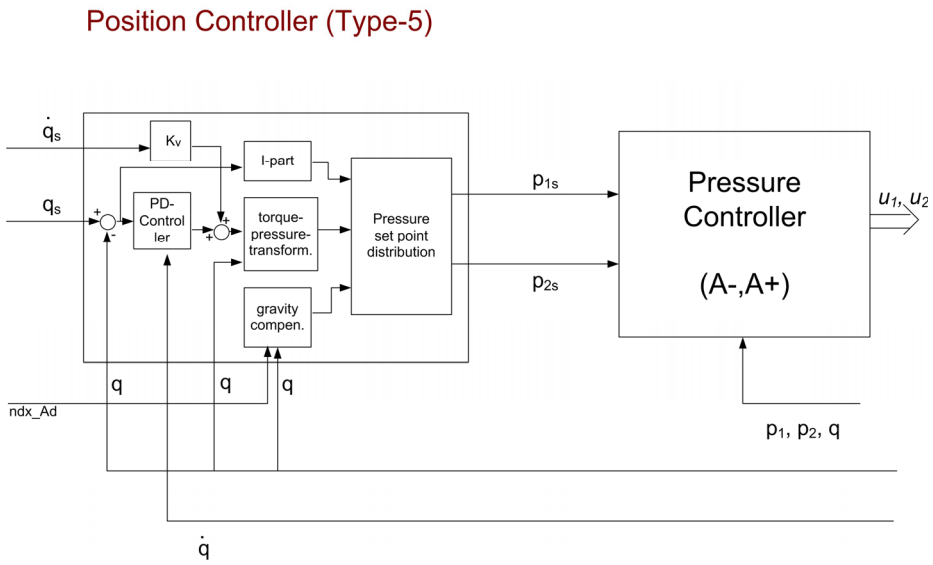

(b) Position Control Scheme

Figure 27. Different Control Schemes

6.3.2. Position control

For the position control in the outer loop, a sliding mode control with time delay estimation (SMCTE) was proposed and successfully tested for a single rotary joint. In the control design, the specific experimentally investigated dynamic model of pneumatic driven FFA was taken into account [85, 86]. In hydraulic case the iterative feedback tuning technique was applied [85]. For pneumatic driven planar robots with two soft fluidic actuators, the SMCTE approach was implemented for decentralized joint position control and shows better results than Fuzzy control, optimized using genetic algorithm [64]. Position control for pneumatic soft-robots

with spatial modular kinematics based on FFA modules is considered in [127]. In addition to decentralized SMCTE position controller the active gravity compensation-based on the quasi-static robot model is used in feed-forward loop to take the weight of robot mechanics into account. Experimental investigations, conducted with different loads for soft-robots with 4 and 6 degrees of freedom (DOF), show the behavior, the quality and the limits of the decentralized control concept with and without active gravity compensation.

6.3.3. Interaction control

The application of different control strategies for physical interaction of pneumatic soft-robots with the environment is studied in [147] by simulation and in [9] also by experiment. For control feedback the current measurements of pressure and joint angle position as well as a force/torque observer based on inverted experimental torque characteristics of FFA are used. Hereby the force sensor abilities of FFAs as of a kind of smart actuators are utilized. An adaptive admittance control with trajectory modification (ACTM) is compared by simulation to an adaptive admittance control with variable stiffness regulation (ACSR) using a model of a planar robot with two rotary joints. Both concepts enable desired force tracking in constraint direction and compliant position control in unconstrained direction. Furthermore the more promising ACSR approach was implemented and validated within an experimental set-up using a planar soft-robot with two FFA joint units by tracking even or lightly curved surfaces without knowledge of the environment stiffness.

7. Inflatable structural elements

Chapter 2.2 showed some examples of how inflatable structures can contribute to compliant robotics. This chapter shows how a modular design can help to integrate inflatable structures in robots independently from the drive concept. The main load cases of robotic structures are bending and torsion. In the shell of inflatable structures we have a state of plane stress. The shell cannot carry significant compressive force. However, when pressurized the shell is pretensioned. Compressive forces thus decrease this pretension in the shell. When the compressive forces overcome the pretension the whole structure deflects and yields the external loads.

The general fabrication process of structural elements is identical to the process described in chapter 3.2.1. The different load cases require different reinforcements in the shell. Two different layers are integrated in the shell in order to carry bending and torsion respectively. The fibers of the braided reinforcement follow the directions of the principal stresses for torsion on the surface of a cylinder as shown in figure 28(a). The reinforcement for pressure stability and bending are are shown in figure 28(b). This second reinforcement layer is a woven fabric tube with radial and axial fiber directions. The relationships between internal pressure and bending or torsional stiffness are presented in figure 28(c) and 28(d). These graphs show how the stiffness can be adjusted depending on the compliance requirements. Each front end of the structural element is equipped with a four screw flange, which allows for easy mounting and pressure sensor integration [36].

8. Flexure hinges in the field of robotics

The combination of flexible fluidic actuators and flexures leads to robotic structures with extraordinary characteristics in terms of weight, compliance, and degree of integration. This

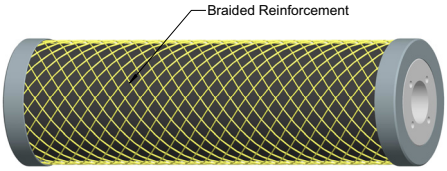

(a) Braided Reinforcement

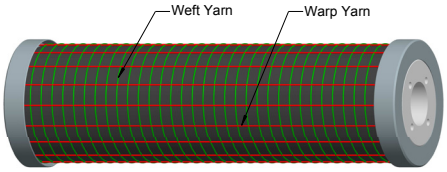

(b) Woven Reinforcement

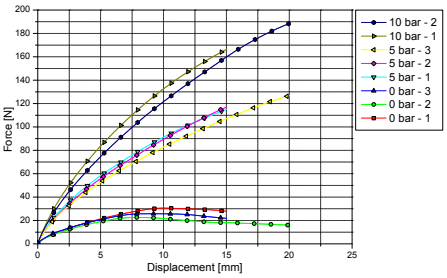

(c) Bending Stiffness of Compliant Structural Element

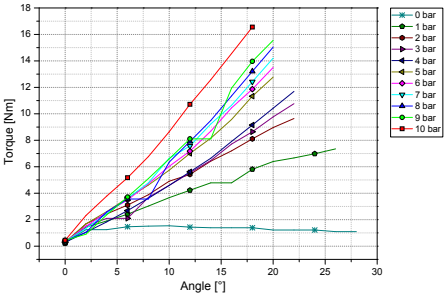

(d) Torsional Stiffness of Compliant Structural Element

Figure 28

section introduces fiber reinforced flexures fabricated in a VARTM-process (Vacuum Assisted Resin Transfer Molding).

A flexure hinge transforms an applied force into a rotary motion due to its different structural stiffnesses. The shorter the flexure length the more precise is the rotating motion. General consideration of beam theory show how the maximum bending stress σ_{max} limits the deflection Δx of the beam [51, 78].

$$\sigma_{max} = \frac{3\Delta x E \frac{h}{2}}{L^2} \tag{11}$$

Given that the desired deflection cannot be changed, the bending stress can only be influenced by the beam's height h and length L. By subdividing the bending beam of a flexure hinge the bending stress stays low without losing structural strength (figure 29).

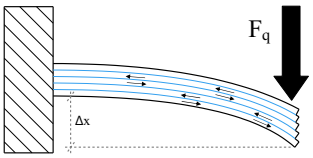

Figure 29. Simplified schematic view of a flexure hinge as a subdivided bending beam

Practically this approach is implemented by using woven fiber tapes to reinforce the bending section. The single fiber filaments represent the subdivided beams. After evaluation of technical fibers UHMWPE-fibers (also know under the brand name DYNEEMA®) have been found to meet the requirements best [36].

Dynamic testing has shown that after 100,000 cycles, no visible damage is present. Static testing has also been described in earlier work [36]. The properties have found to be extraordinary with operating loads up to $100N$ and a maximum carrying capacity of over $3,000N$. The enhanced fabrication process for flexures allows for the production of single-acting (mass $9.1\,g$) and double-acting (mass $11.6\,g$) drives with full integration of the flexible fluidic actuator as well as the position sensor as described in [36]. Figure 30 shows the different joint-modules. These modules now can be freely combined as shown in figure 35.

(a) Single-Acting composite flexure drive

(b) Double-Acting composite flexure drive

Figure 30. Different Designs for Composite Flexure Drives in Robots

9. Applications

A large amount of robotic systems with flexible fluidic actuators have been developed over the last ten years. This is represented in many publications and patents [35, 65, 66, 108–111, 113–116]. These systems come from fields such as prosthetics, orthotics, medical devices as well as humanoid robotics and automation. Here some of the latest developments in the fields of vulcanized and HF-welded actuators are presented.

9.1. Robotic systems based on vulcanized FFAs

9.1.1. Modular flexible fluidic drive elements

These drives are based on the $\varnothing 36\,mm$ actuator. Integrated in the modules are the valves and one position sensor (AS5045-austriamicrosystems) as well as two pressure sensors (MS5803-14BA-measurement specialties) (figure 31).

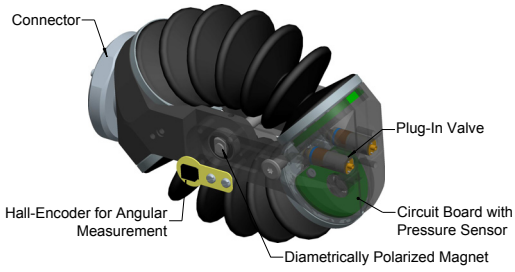

Figure 31. Highly Integrated Flexible Fluidic Drive Module

The modules can be combined in several parallel and serial configurations. Hence the torque-angle characteristics can be varied and adjusted to the case of operation, which is presented in figure 32-34.

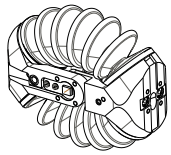

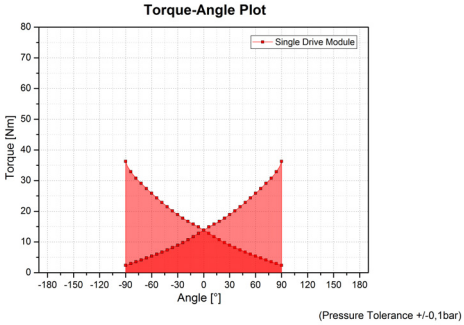

Figure 32. Single Drive Module

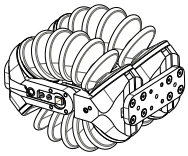

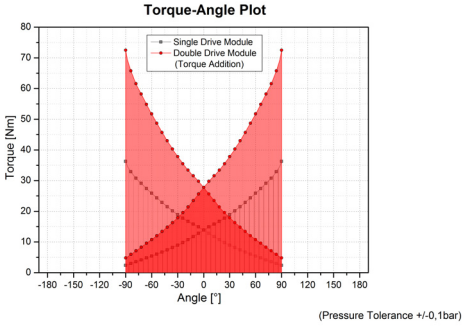

Figure 33. Double Module - Parallel Configuration

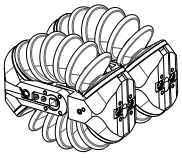

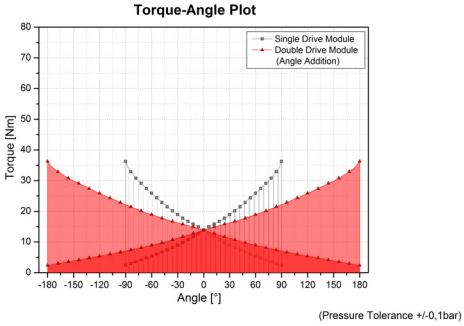

Figure 34. Double Module - Serial Configuration

9.1.2. Three-fingered composite gripper

The fiber reinforced flexure hinges are combined to form a three-fingered gripper as shown in figure 35. The base of this gripper is built of three double-acting flexure drives. Each finger is designed with two single acting flexure drives. The base of the gripper has three main positions. These positions are for spherical, cylindrical and precision grasping (figure 35). However, the compliance of the gripper allows a large variety of grasps. Figure 36 shows the taxonomy of the different grasps. The total weight of the gripper is 400 g. Each finger has a length of 140 mm.

(a) Overview (b) Spherical (c) Parallel (d) Precision

Figure 35. Main Base Positions of the Composite Gripper

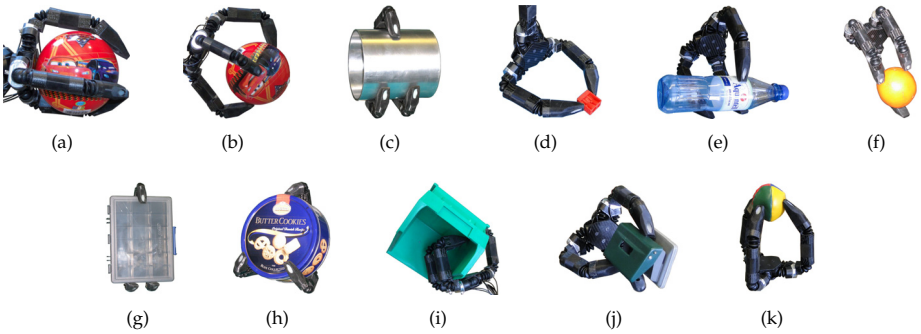

(a) (b) (c) (d) (e) (f)

(g) (h) (i) (j) (k)

Figure 36. Grasp Taxonomy of the Composite Gripper

9.1.3. Lightweight Robotic Arm (LRA)

The drive modules, compliant structural elements, and the composite gripper have modular interfaces and can be combined freely. To evaluate the whole system a 6 DOF arm has been designed and built (figure 37). The proximal joint consists of two combined drive modules in parallel configuration. The weight of the whole arm is 3.45 kg and has a total length of 735 mm.

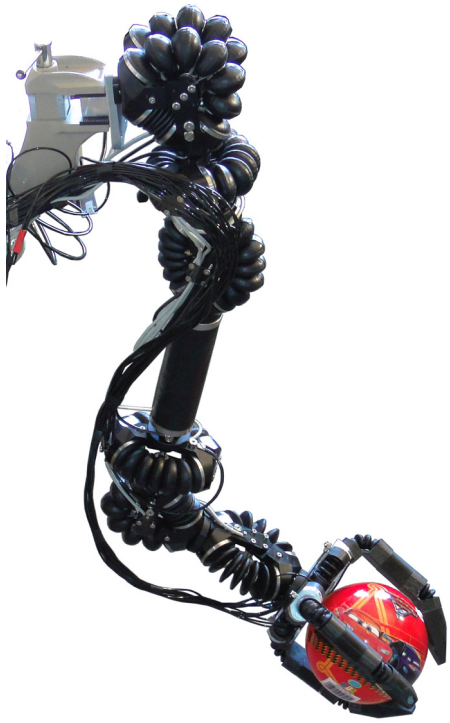

Figure 37. Lightweight Robotic Arm

9.2. Robotic systems based on HF-welded FFAs

The most recent achievements concerning HF-welded actuators are in the field of orthotics. The wide range of design possibilities of this manufacturing technology enable tailored geometries. Figure 38(a) shows an active elbow orthesis actuated with HF-welded FFAs.

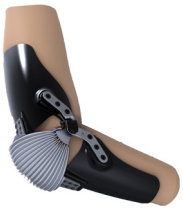

(a) Elbow Orthesis

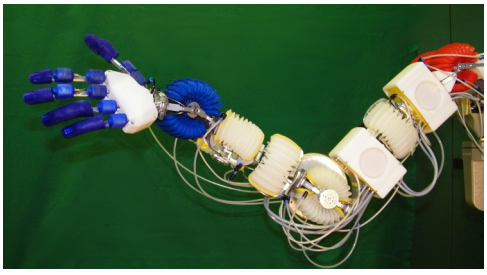

(b) 6-DOF GPA-Arm

Figure 38. Systems with HF-welded Actuators

The GPA modules also allow modular combination. Figure 38(b) shows a complete 6-DOF arm including two controller boxes and an anthropomorphic hand. The controller boxes provide valves, pressure sensors and microcontrollers to operate the whole arm independently. The whole arm-hand system has a weight of 3.2kg and a overall length of 620mm.

10. Conclusions

The future of robotics will require more and more inherent compliance. Inherent compliance can only be achieved by integrating elastic elements in the drive chain of a robotic system. Flexible Fluidic Actuators can be an appropriate solution for this problem. FFAs exhibit inherent compliance no matter if they are operated pneumatically or hydraulically. A big advantage is that FFAs do not require any transmission elements to create a rotary motion. The high torque-to-weight ratio make them suitable drives for robotics, prosthetics, orthotics, and general automation tasks. The modularity allows easy implementation of various kinematics, either for grippers and/or arms. The fluidic operation principle also make FFAs a very promising drive system for under water and deep sea operation. The challenges regarding fabrication and fatigue resistance of FFAs have been solved. The modeling and control approaches are very promising and the required control infrastructure will definitely shrink with future valve technologies and high-performance micro controllers.

Acknowledgments

The authors would like to thank all contributors and project partners. Especially we thank Maika Torge (Institute for Applied Materials/KIT) for her support regarding SEM analysis and tensile testing as well as Stefan Griebel (BMTI/TU Ilmenau) for his support regarding hyperelastic material modeling. This work was supported by the German Federal Ministry of Education and Research (BMBF) within the joint research project PortaSoR, Grants 16SV2290 - 16SV2294.

Author details

I. Gaiser, R. Wiegand, O. Ivlev, A. Andres, H. Breitwieser, S. Schulz and G. Bretthauer
Karlsruhe Institute of Technology (KIT), Institute for Applied Computer Science/Automation (AIA), Institute for Applied Computer Science (IAI); FWBI Friedrich-Wilhelm-Bessel-Institute Research Company and University of Bremen, Institute of Automation (IAT), Germany

11. References

[1] A. Kargov, T. Werner, C. P. S. S. [2008]. Development of a miniaturised hydraulic actuation system for artificial hands, *Sensors and Actuators A: Physical* 141: 548–557.
[2] Abele, G. . F. [1970]. *Arbeitsmappe System 70*, Zechner und Hüthig Verlag.
[3] Akhtar, S., De, P. P. & De, S. K. [1986]. Short fiber-reinforced thermoplastic elastomers from blends of natural rubber and polyethylene, *J. Appl. Polym. Sci.* 32(5): 5123–5146. URL: *http://dx.doi.org/10.1002/app.1986.070320530*
[4] Alami, R., Albu-Schaeffer, A., Bicchi, A., Bischoff, R., Chatila, R., Luca, A. D., Santis, A. D., Giralt, G., Guiochet, J., Hirzinger, G., Ingrand, F., Lippiello, V., Mattone, R.,

Powell, D., Sen, S., Siciliano, B., Tonietti, G. & Villani, L. [2006]. Safe and dependable physical human-robot interaction in anthropic domains: State of the art and challenges, *in* A. Bicchi & A. D. Luca (eds), *Procceedings IROS Workshop on pHRI - Physical Human-Robot Interaction in Anthropic Domains*, Beijing, China.

[5] Andorf, P., Franz, D., Lieb, A., Upper, G. & Guttropf, W. [1976]. Robot finger. URL: *http://www.freepatentsonline.com/3981528.html*

[6] Antonelli, K. & Immega, G. [1997]. An extensible robotic tentacle, *Industrial Robot: An International Journal* 24(6): 423 – 427.

[7] Baer, J. I. [1967]. Material handling apparatus and the like. URL: *http://www.freepatentsonline.com/3343864.html*

[8] Baer, J. I. [1975]. Fluid motor and material handling apparatus and the like utilizing same. URL: *http://www.freepatentsonline.com/RE28663.html*

[9] Baiden, D., Bartuszies, S. & Ivlev, O. [2012]. Position control of soft-robots with rotary-type pneumatic actuators, *7th German Conf. On Robotics (Robotik 2012)*, Munich, Germany, pp. 405–410.

[10] Bayerkohler, I. L. [1957]. Pneumatic bellows type jacks. URL: *http://www.freepatentsonline.com/2804118.html*

[11] Bögelsack, G., Karner, M. & Schilling, C. [2000]. On technomorphic modelling and classification of biological joints, *Theory in Biosciences* 119(2): 104–121. URL: *http://dx.doi.org/10.1007/s12064-000-0007-3*

[12] Bicchi, A. & Tonietti, G. [2004]. Fast and "soft-arm" tactics (robot arm design), *Robotics Automation Magazine, IEEE* 11(2): 22 – 33.

[13] Bousso, D. E. [1970]. Bellows devices. URL: *http://www.freepatentsonline.com/3495502.html*

[14] Brown, E., Rodenberg, N., Amend, J., Mozeika, A., Steltz, E., Zakin, M., Lipson, H. & Jaeger, H. [2010]. Universal robotic gripper based on the jamming of granular material, *Proceedings of the National Academy of Sciences (PNAS)*, Vol. 107, pp. 18809–18814.

[15] Bubic, F. R. [1992]. Flexible robotic links and manipulator trunks made thereform. URL: *http://www.freepatentsonline.com/5080000.html*

[16] CLAUS, H.-J. [2003]. Fluid-operated actuator has contraction hose fitting with at least one long contraction hose which can be pressurized by operating fluid.

[17] ContiTech AG [2011]. ContiTech Luftfedersysteme. URL: *http://213.164.133.30/lufecatalog/*

[18] Craig, P. S. & Fisher, J. A. [1989]. Grappling device. URL: *http://www.freepatentsonline.com/4815782.html*

[19] Daerden, F. [1999]. *Conception and Realization of Pleated Pneumatic Artificial Muscles and their Use as Compliant Actuation Elements*, PhD thesis, Vrije Universiteit Brussel.

[20] Daerden, F. & Lefeber, D. [2000]. Pneumatic artificial muscles: actuators for robotics and automation, *European journal of Mechanical and Environmental Engineering* 47: 10–21.

[21] Daerden, F. & Lefeber, D. [2001]. The concept and design of pleated pneumatic artificial muscles, *International Journal of Fluid Power* 2(3): 41–50.

[22] de Lavaud, D. S. [1929]. Vorrichtung zur Erzeugung eines Über- oder Unterdruckes in Gasen oder Flüssigkeiten.

[23] DeLepeleire, G. A. [1974]. Bag diaphragms and bag diaphragm operated air dampers. URL: *http://www.freepatentsonline.com/3804364.html*

[24] Edsinger, A. [2011]. Meka robotics. URL: *http://mekabot.com/MEKA_brochure02.pdf*

[25] Erickson, Joel R. (7636 Circle Hill Dr., O. C. . [2001]. Artificial muscle actuator assembly. URL: *http://www.freepatentsonline.com/6223648.html*

[26] Eurovinil S.P.A. [2011]. *Aufblasbares Zelt TPSE*, Eurovinil S.P.A.
[27] Ewing [1973]. Flexible actuator. URL: *http://www.freepatentsonline.com/3713685.html*
[28] Fang, H. & Lou, M. C. [2004]. Analytical characterization of space inflatable structures - an overview, *AIAA/ASME/ASC Structures, SDM Conference*, St. Louis, MO.
URL: *http://hdl.handle.net/2014/16760*
[29] Festo AG & Co KG [1999]. Betätigungseinrichtung.
[30] Festo AG & Co. KG [2009]. *Fluidic Muscle DMSP/MAS*.
[31] Fleury, L. A. [1919]. Pneumatic jack.
[32] Frank, B. [1924]. Pneumatic incline. URL: *http://www.freepatentsonline.com/1493729.html*
[33] Freeland, R. E., Bilyeu, G. D., Veal, G. R., Steiner, M. D. & Carson, D. E. [1997]. Large inflatable deployable antenna flight experiment results, *Acta Astronautica* 41(4-10): 267 – 277. Developing Business.
URL: *http://www.sciencedirect.com/science/article/pii/S0094576598000575*
[34] Fuchs, G. [1994]. Faltenbalg.
[35] Gaiser, I., Pylatiuk, C., Schulz, S., Kargov, A., Oberle, R. & Werner, T. [2009]. The FLUIDHAND III: A Multifunctional Prosthetic Hand, *JPO Journal of Prosthetics & Orthotics* 21: 91–96.
[36] Gaiser, I., Schulz, S., Breitwieser, H. & Bretthauer, G. [2010]. Enhanced flexible fluidic actuators for biologically inspired lightweight robots with inherent compliance, *Robotics and Biomimetics (ROBIO), 2010 IEEE International Conference on*, pp. 1423 –1428.
[37] Giesler, J. V. [1932]. Attachment of heads to bellows.
URL: *http://www.freepatentsonline.com/1870904.html*
[38] Griebel, S., Fiedler, P., Streng, A., Haueisen, J. & Zentner, L. [2010]. Medical sensor placement with a screw motion, *Actuator 10 / International Conference on New Actuators*, Bremen, Germany, pp. 1047–1050.
[39] Gudo, M. [2002]. The development of the critical theory of evolution: The scientific career of wolfgang f. gutmann, *Theory in Biosciences* 121(1): 101–137.
URL: *http://dx.doi.org/10.1078/1431-7613-00052*
[40] Gudo, M. & Grasshoff, M. [2002]. The origin and early evolution of chordates: The hydroskelett-theorie and new insights towards a metameric ancestor, *Palaeobiodiversity and Palaeoenvironments* 82(1): 325–345.
URL: *http://dx.doi.org/10.1007/BF03043792*
[41] Gutmann, W. F. [1966]. *Zu Bau und Leistung von Tierkonstruktionen (4-6)*, Abhandlungen der Senckenbergischen Naturforschenden Gesellschaft ; 510Senckenberg am Meer ; 238, Frankfurt a. M.
[42] Gutmann, W. F. [1972]. *Die Hydroskelett-Theorie : AbriSS der Coelomaten-Herleitung von einer metameren Vorläufer-Konstruktion*, Aufsätze und Reden der Senckenbergischen Naturforschenden Gesellschaft ; 21, Kramer, Frankfurt a. M.
[43] Haddadin, S., Albu-Schaeffer, A. & Hirzinger, G. [2007]. Safety evaluation of physical human-robot interaction via crash-testing.
URL: *http://citeseerx.ist.psu.edu/viewdoc/summary?doi=10.1.1.149.1487*
[44] Haddadin, S., Albu-Schaffer, A., Frommberger, M., Rossmann, J. & Hirzinger, G. [2009a]. The dlr crash report : Towards a standard crash-testing protocol for robot safety - part i: Results, *Robotics and Automation, 2009. ICRA '09. IEEE International Conference on*, pp. 272 –279.
[45] Haddadin, S., Albu-Schaffer, A., Frommberger, M., Rossmann, J. & Hirzinger, G. [2009b]. The dlr crash report: Towards a standard crash-testing protocol for robot

safety - part ii: Discussions, *Robotics and Automation, 2009. ICRA '09. IEEE International Conference on*, pp. 280 –287.
[46] Haegele, M., Neugebauer, J. & Schraft, R. [2001]. From robots to robot assistants, *32nd ISR(International Symposium on Robotics)*.
[47] Hennequin, J. R. & Fluck, P. [1990]. Motorized joint.
URL: *http://www.freepatentsonline.com/4944755.html*
[48] Henriksen, T. K. [2008]. Trends in materials requirements in spacecraft structures and mechanisms, *Materials KTN 2nd Annual General Meeting*.
[49] Hertel, B. [1984]. Personnel qualification and work structuring in robot-automated manufacturing systems - exemplified by the application of industrial robots for body shell assembly at audi, ingolstadt, *in* N. Martensson (ed.), *Proceedings on 14th International Symposium on Industrial Robots*, Gothenburg, Sweden.
[50] Hirzinger, G., Sporer, N., Albu-Schäffer, A., Hahnle, M., Krenn, R., Pascucci, A. & Schedl, M. [2002]. DLR's torque-controlled light weight robot III. Are we reaching the technological limits now?, *Robotics and Automation, 2002. Proceedings. ICRA '02. IEEE International Conference on*, Vol. 2, pp. 1710 – 1716.
[51] Howell, L. [2002]. *Compliant Mechanisms*, John Wiley & Sons INC.
[52] IFR - International Federation of Robotics [2010a]. Executive summary of world robotics 2010, *Technical report*, IFR - International Federation of Robotics.
[53] IFR - International Federation of Robotics [2010b]. Serviceroboter etablieren sich erfolgreich, *Technical report*, IFR - International Federation of Robotics.
[54] IFR - International Federation of Robotics [2011a]. Ifr - charts for press, servicerobotik 2011, *Technical report*, IFR - International Federation of Robotics.
[55] IFR - International Federation of Robotics [2011b]. Ifr: Allzeithoch für die roboterindustrie - das kräftige wachstum der roboterverkäufe setzt sich fort, *Technical report*, IFR - International Federation of Robotics.
[56] IFR - International Federation of Robotics [2011c]. Professionelle service roboter - einsatz im militärischen bereich und der landwirtschaft überwiegen, *Technical report*, IFR - International Federation of Robotics.
[57] Ilievski, F., Mazzeo, A. D., Shepherd, R. F., Chen, X. & Whitesides, G. M. [2011]. Soft robotics for chemists, *Angewandte Chemie International Edition* 50(8): 1890–1895.
URL: *http://dx.doi.org/10.1002/anie.201006464*
[58] Immega, G. & Kukolj, M. [1990]. Axially contractable actuator.
URL: *http://www.freepatentsonline.com/4939982.html*
[59] *Industrieroboter- Sicherheitanforderungen - Teil 1, DIN EN ISO 10218-1* [2009].
[60] *Industrieroboter - Sicherheitanforderungen - Teil 2, DIN EN ISO 10218-2* [2008].
[61] Ivlev, O. [2009]. Soft fluidic actuators of rotary type for safe physical human-machine interaction, *Rehabilitation Robotics, 2009. ICORR 2009. IEEE International Conference on*, pp. 1 –5.
[62] Johnston, L. B. [1965]. Fluid actuated displacement and positioning system.
URL: *http://www.freepatentsonline.com/3202061.html*
[63] Jones, J. A. [2001]. Inflatable robotics for planetary applications, *Proceeding of the 6th International Symposium on Artificial Intelligence and Robotics & Automation in Space: i-SAIRAS*, Canadian Space Agency, St-Hubert, Quebec, Canada.
[64] Jordan, M., Pietrusky, D., Mihajlov, M. & Ivlev, O. [2009]. Precise position and trajectory control of pneumatic soft-actuators for assistance robots and motion therapy devices, *Rehabilitation Robotics, 2009. ICORR 2009. IEEE International Conference on*, pp. 663 –668.

[65] Kargov, A., Asfour, T., Pylatiuk, C., Oberle, R., Klosek, H., Schulz, S., Regenstein, K., Bretthauer, G. & Dillmann, R. [2005]. Development of an anthropomorphic hand for a mobile assistive robot, *Proceedings of the 9th International Conference on Rehabilitation Robotics*, ICORR, pp. 182–186.

[66] Kargov, A., Werner, T., Pylatiuk, C. & Schulz, S. [2008]. Development of a miniaturised hydraulic actuation system for artificial hands, *Sensors and Actuators A: Physical* 141(2): 548 – 557.
URL: *http://www.sciencedirect.com/science/article/B6THG-4PXDM21-4/2/56ea17517c8be38c771afc6d2c49b310*

[67] Karwowski, W., Rahimi, M., Parsaei, H., Amarnath, B. R. & Pongpatanasuegsa, N. [1991]. The effect of simulated accident on worker safety behavior around industrial robots, *International Journal of Industrial Ergonomics* 7(3): 229 – 239.
URL: *http://www.sciencedirect.com/science/article/B6V31-481DT49-4H/2/f5d48f31d92b445ab7192e795b1d2ffd*

[68] Khatib, O., Yokoi, K., Brock, O., Chang, K. & Casal, A. [1999]. Robots in human environments, *Robot Motion and Control, 1999. RoMoCo '99. Proceedings of the First Workshop on*, pp. 213 –221.

[69] Kimura, H., Kajimura, F., Maruyama, D., Koseki, M. & Inou, N. [2006]. Flexible hermetically-sealed mobile robot for narrow spaces using hydrostatic skeleton driving mechanism, *Intelligent Robots and Systems, 2006 IEEE/RSJ International Conference on*, pp. 4006 –4011.

[70] Kleinknecht, H., Schuch, A. & Degen, I. [2000]. Process for the production of masterbatches containing short fibres or pulps.
URL: *http://www.freepatentsonline.com/6160039.html*

[71] Konishi, S., Kawai, F. & Cusin, P. [2001]. Thin flexible end-effector using pneumatic balloon actuator, *Sensors and Actuators A: Physical* 89(1-2): 28 – 35.
URL: *http://www.sciencedirect.com/science/article/B6THG-42DX434-5/2/0f8148b596cfdea63ca49836b9dde497*

[72] Koren, Yoram (Ann Arbor, M. & Weinstein, Yechiel (Misgav, I. [1991]. Inflatable structure. URL: *http://www.freepatentsonline.com/5065640.html*

[73] Kukolj, M. [1985]. Axially contractable actuator.

[74] Larsson, Ove (Gothenburg, S. [1988]. Flexible actuator.
URL: *http://www.freepatentsonline.com/4777868.html*

[75] Lens, T., Kunz, J., Trommer, C., Karguth, A. & von Stryk, O. [2010]. Biorob-arm: A quickly deployable and intrinsically safe, light- weight robot arm for service robotics applications, *41st International Symposium on Robotics (ISR 2010) / 6th German Conference on Robotics (ROBOTIK 2010)*, Munich, Germany, pp. 905–910.

[76] Lewis, D. J. [1974]. Fiber reinforced inflatable restraining band for vehicles. URL: *http://www.freepatentsonline.com/3830519.html*

[77] Lewis, J. [1847]. Car spring.
URL: *http://www.freepatentsonline.com/0004965.html*

[78] Lobontiu, N. [2003]. *Compliant mechanisms : design of flexure hinges*, CRC Press, Boca Raton, Fla. [u.a.]. Includes bibliographical references and index.
URL: *http://www.gbv.de/dms/ilmenau/toc/350071101.PDF*

[79] Lou, M. C. [2000]. Development and application of space inflatable structures, *22"d International Symposium on Space Technology and Science Jet Propulsion Laboratory, CaliforniaIn stitute of Technology*, Pasadena, CA, USA.

[80] Malloy, H. C. [1929]. Method of producing expansible collapsible elements.
URL: *http://www.freepatentsonline.com/1698164.html*
[81] Marette, R. T. [1961]. Actuator.
URL: *http://www.freepatentsonline.com/2991763.html*
[82] Marshall Space Flight Center, A. [2010]. Inflatable tubular structures rigidized with foams, *Technical report*, Marshall Space Flight Center, Alabama.
[83] Maruyama, D., Kimura, H., Koseki, M. & Inou, N. [2010]. Driving force and structural strength evaluation of a flexible mechanical system with a hydrostatic skeleton, *Journal of Zhejiang University - Science A* 11: 255–262. 10.1631/jzus.A000030.
URL: *http://dx.doi.org/10.1631/jzus.A000030*
[84] McMahan, W., Chitrakaran, V., Csencsits, M., Dawson, D., Walker, I., Jones, B., Pritts, M., Dienno, D., Grissom, M. & Rahn, C. [2006]. Field trials and testing of the octarm continuum manipulator, *Robotics and Automation, 2006. ICRA 2006. Proceedings 2006 IEEE International Conference on*, pp. 2336 –2341.
[85] Mihajlov, M. [2008]. *Modelling and Control Strategies for Inherently Compliant Fluidic Mechatronic Actuators with Rotary Elastic Chambers*, PhD thesis, Institute of Automation, University of Bremen, Bremen, Germany. ISBN 978-3-8322-7275-3.
[86] Mihajlov, M., Hubner, M., Ivlev, O. & Graser, A. [2006]. Modeling and control of fluidic robotic joints with natural compliance, *Computer Aided Control System Design, 2006 IEEE International Conference on Control Applications, 2006 IEEE International Symposium on Intelligent Control, 2006 IEEE*, pp. 2498 –2503.
[87] Mihajlov, M., Ivlev, O. & Gräser, A. [2008]. Modelling and identification for control design of compliant fluidic actuators with rotary elastic chambers: Hydraulic case study, *17th IFAC World Congress*, Seoul Korea.
[88] Monroe, John W. (Warren, M. [1994]. Jointed assembly actuated by fluid pressure.
URL: *http://www.freepatentsonline.com/5351602.html*
[89] Morin, A. H. [1953]. Elastic diaphragm.
URL: *http://www.freepatentsonline.com/2642091.html*
[90] Morse, R. V. [1938]. Pneumatic jack.
URL: *http://www.freepatentsonline.com/2140325.html*
[91] Mårtensson, L. [1987]. Interaction between man and robots, *Robotics* 3(1): 47 – 52. Special Issue: Industrial Robotics.
URL: *http://www.sciencedirect.com/science/article/B756Y-480TX1T-N/2/e9dc7e14bd276f81846f0ac477638069*
[92] Negishi, Koichi (Kodaira, J. [1991]. Double-acting flexible wall actuator.
URL: *http://www.freepatentsonline.com/5067390.html*
[93] Nicolaisen, P. [1987]. Safety problems related to robots, *Robotics* 3(2): 205 – 211. Special Issue: Sensors.
URL: *http://www.sciencedirect.com/science/article/B756Y-4808M3V-9/2/39a6988a29109bc9bafa999095e31aa2*
[94] Oñate, E. & Kröplin, B. (eds) [2008]. *Textile Composites and Inflatable Structures II*, Springer.
[95] Orndorff, R. L. [1971]. Gripping device.
URL: *http://www.freepatentsonline.com/3601442.html*
[96] Patterson, J. M. [1935]. Lifting jack. URL: *http://www.freepatentsonline.com/2001744.html*
[97] PAUL, L. J. [1998]. Inflatable wall for sealing manholes or pipes to test for water tightness, fr2751006, *Technical report*, PRONAL.

[98] Paynter, H. M. [1974]. Tension actuated pressurized gas driven rotary motors.
URL: *http://www.freepatentsonline.com/3854383.html*

[99] Paynter, Henry M. (35 Scotland Rd., R. M. . [1978]. Fluid-driven torsional operators for turning rotary valves and the like.
URL: *http://www.freepatentsonline.com/4108050.html*

[100] Paynter, Henry M. (35 Scotland Rd., R. M. . [1988a]. High pressure fluid-driven tension actuators and method for constructing them.
URL: *http://www.freepatentsonline.com/4751869.html*

[101] Paynter, Henry M. (35 Scotland Rd., R. M. . [1988b]. Hyperboloid of revolution fluid-driven tension actuators and method of making.
URL: *http://www.freepatentsonline.com/4721030.html*

[102] Paynter, Henry M. (Pittsford, V. [1992]. All-elastomer fluid-pressure-actuatable twistors and twistor drive assemblies.
URL: *http://www.freepatentsonline.com/5090297.html*

[103] Prior, S., Warner, P., White, A., Parsons, J. & Gill, R. [1993]. Actuators for rehabilitation robots, *Mechatronics* 3(3): 285 – 294. Special Issue Robot Actuators.
URL: *http://www.sciencedirect.com/science/article/B6V43-47YVPRC-3/2/0a2fb2c92d4ec09d6493c32cdf2ed09e*

[104] Rybski, M., Shoham, M. & Grossman, G. [1996]. Robotic manipulators based on inflatable structures, *Robotics and Computer-Integrated Manufacturing* 12(1): 111 – 120.
URL: *http://www.sciencedirect.com/science/article/B6V4P-3VV72YC-C/2/ad2533e8ae922da2adf9e131f35cf7f8*

[105] Salomonski, N., Shoham, M. & Grossman, G. [1995]. Light robot arm based on inflatable structure, *CIRP Annals - Manufacturing Technology* 44(1): 87–90.
URL: *http://www.sciencedirect.com/science/article/B8CXH-4P3DTXT-P/2/ce613ff549a49cb798f0d515bbc42c0f*

[106] Sanan, S., Moidel, J. & Atkeson, C. [2009]. Robots with inflatable links, *Intelligent Robots and Systems, 2009. IROS 2009. IEEE/RSJ International Conference on*, pp. 4331–4336.

[107] Schneider, E. [1993]. Air spring having an elastomeric air-spring flexible member.
URL: *http://www.freepatentsonline.com/5269496.html*

[108] Schulz, S. [2000]. Wurmförmiger Arbeitsmechanismus.

[109] Schulz, S. [2004a]. *Eine neue Adaptiv-Hand-Prothese auf der Basis flexibler Fluidaktoren*, PhD thesis, Universität Karlsruhe (TH).
URL: *http://books.google.de/books?id=A9VWAgAACAAJ*

[110] Schulz, S. [2004b]. Vorrichtung mit fluidischem schwenkantrieb.

[111] Schulz, S. [2005]. Fluidischer antrieb.

[112] Schulz, S., Pylatiuk, C. & Bretthauer, G. [1999a]. A new class of flexible fluidic actuators and their applications in medical engineering, *Automatisierungstechnik* 8: 390–395.

[113] Schulz, S., Pylatiuk, C. & Bretthauer, G. [1999b]. A new class of flexible fluidic actuators and their applications in medical engineering, *at-Automatisierungstechnik* 47(8): 390–395.

[114] Schulz, S., Pylatiuk, C., Kargov, A., Gaiser, I., Schill, O., Reischl, M., Eck, U. & Rupp, R. [2009]. Design of a hybrid powered upper limb orthosis, *Proc., World Congress Medical Physics and Biomedical Engineering*, München.

[115] Schulz, S., Pylatiuk, C., Kargov, A., Oberle, R., Klosek, H., Werner, T., RöSSler, W., Breitwieser, H. & Bretthauer, G. [2005]. Fluidically driven robots with biologically inspired actuators, *Proc. of the 8th International Conference on Climbing and Walking Robots (CLAWAR)*, London, UK, p. 39.

[116] Schulz, S., Pylatiuk, C., Reischl, M., Martin, J., Mikut, R. & Bretthauer, G. [2005]. A hydraulically driven multifunctional prosthetic hand, *Robotica* 23(3): 293–299.
[117] Shin, D., Khatib, O. & Cutkosky, M. [2009]. Design methodologies of a hybrid actuation approach for a human-friendly robot, *Robotics and Automation, 2009. ICRA '09. IEEE International Conference on*, pp. 4369 –4374.
[118] Shoval, S. & Shoham, M. [2001]. Sensory redundant parallel mobile mechanism, *Conference on Robotics and Automation, 2001. Proceedings 2001 ICRA. IEEE International*, Vol. 3, pp. 2273 – 2278 vol.3.
[119] Sigmon, J. W. [1976]. Rotary motion valve and actuator.
URL: *http://www.freepatentsonline.com/3977648.html*
[120] Staines, A. J. [1962]. Sheet lifting device.
URL: *http://www.freepatentsonline.com/3039767.html*
[121] Stienenw, A., Hekman, E., ter Braak, H., Aalsma, A., van der Helm, F. & van der Kooij, H. [2010]. Design of a rotational hydroelastic actuator for a powered exoskeleton for upper limb rehabilitation, *Biomedical Engineering, IEEE Transactions on* 57(3): 728 –735.
[122] Suzumori, K. [1992]. Gripping actuator with independently flexible cylinders.
URL: *http://www.freepatentsonline.com/5156081.html*
[123] Suzumori, K. [1995]. Actuator with flexible cylinders.
URL: *http://www.freepatentsonline.com/5385080.html*
[124] Suzumori, K. [1996]. Elastic materials producing compliant robots, *Robotics and Autonomous Systems* 18: 135–140(6).
[125] Suzumori, K., Endo, S., Kanda, T., Kato, N. & Suzuki, H. [2007]. A bending pneumatic rubber actuator realizing soft-bodied manta swimming robot, *IEEE International Conference on Robotics and Automation*, Roma, Italy, pp. 4975 –4980.
[126] Suzumori, K., Iikura, S. & Tanaka, H. [1992]. Applying a flexible microactuator to robotic mechanisms, *Control Systems Magazine, IEEE* 12(1): 21 –27.
[127] Taghia, J., Wilkening, A. & Ivlev, O. [2012]. Position control of soft-robots with rotary-type pneumatic actuators, *7th German Conf. On Robotics (Robotik 2012)*, Munich, Germany, pp. 399–404.
[128] Takagi, Takeo (Yokohama, J. & Sakaguchi, Yuji (Kawasaki, J. [1986]. Pneumatic actuator for manipulator.
URL: *http://www.freepatentsonline.com/4615260.html*
[129] Tillett, N., Vaughan, N. & Bowyer, A. [1994]. An improved flexible pneumatic joint for horticultural robots, *Mechatronics* 4(7): 653 – 671.
URL: *http://www.sciencedirect.com/science/article/B6V43-480TWR6-T/2/59208c93bf4b07b4417f3c73d0a3efd1*
[130] Trivedi, D., Rahn, C. D., Kier, W. M. & Walker, I. D. [2008]. Soft robotics: Biological inspiration, state of the art, and future research, *Applied Bionics and Biomechanics* 5(3): 99–117.
URL: *http://www.informaworld.com/10.1080/11762320802557865*
[131] Tsimpris, C., Wartalski, J., Ferradino, A. & Vanderbilt, R. [2001]. Compounding with para-aramid fiber engineered elastomers., *Rubber World* 224(1): 35.
URL: *http://www.redi-bw.de/db/ebsco.php/search.ebscohost.com/login.aspx?direct=true&db=buh&AN=4385775&site=ehost-live*
[132] VanBlaricum, M. L., Reilley, J., Gilbert, M. A. & VanBlaricum Jr., G. F. [1999]. Quick feasibility demonstration for an inflatable antenna system in space, *Proceedings of the*

Ninth Annual DARPA Symposium on Photonic Systems for Antenna Applications, Monterey, CA.

[133] Vaughen, J. F. [1993]. Structure for an inflatable lift device.
URL: *http://www.freepatentsonline.com/5178367.html*

[134] Vetter GmbH [2011]. *VETTER Rettungstechnik*, Vetter GmbH.
URL: *www.vetter.de*

[135] Voisembert, S., Riwan, A., Mechbal, N. & Barraco, A. [2011]. A novel inflatable robot with constant and continuous volume, *Robotics and Automation (ICRA), 2011 IEEE International Conference on*, pp. 5843 –5848.

[136] Widmer, S. W. [1985]. Air bag jack.
URL: *http://www.freepatentsonline.com/4560145.html*

[137] Wilkening, A., Mihajlov, M. & Ivlev, O. [2010]. Model-based pressure and torque control for innovative pneumatic soft-actuators, *Proc. of 7th Int. Conf. on Fluid Power (7th IFK)*, Vol. 4, Aachen, Germany, pp. 291–302.

[138] Williamson, M. M. [1995]. Series elastic actuators, *Technical Report 1524*, MIT, Artificial Iintelligence Laboratory.

[139] Wilson, James F. (Durham, N. [1988]. Fluid actuated limb.
URL: *http://www.freepatentsonline.com/4792173.html*

[140] Wolf, S. & Hirzinger, G. [2008]. A new variable stiffness design: Matching requirements of the next robot generation, pp. 1741 –1746.

[141] Woods, J. E. [1957]. Mechanical transducer with expansible cavity.
URL: *http://www.freepatentsonline.com/2789580.html*

[142] Wypych, G. [2000]. *Handbook of Fillers - A Definitive User's Guide and Databook (2nd Edition)*, ChemTec Publishing.
URL: *http://www.knovel.com/web/portal/browse/display?_EXT_KNOVEL_DISPLAY_ bookid =1011*

[143] Yarlott, J. M. [1972]. Fluid actuator.
URL: *http://www.freepatentsonline.com/3645173.html*

[144] Yoon, C. S., Lee, E. M., Jang, M. S., Song, C. K., Kang, C. Y., Kim, K. H. & Kim, B. K. [2008]. High-frequency welding of thermoplastic lldpe/pa6/pe-g-mah ternary blends, *Journal of Applied Polymer Science* 109: 3355–3360.

[145] Zentner, L. & Böhm, V. [2007]. Nachgiebige monolithische fluidisch angetriebene aktuatoren mit neuartigem verformungsverhalten, *Technische Mechanik* 27(1): 18–27.

[146] Zentner, L., Böhm, V. & Minchenya, V. [2009]. On the new reversal effect in monolithic compliant bending mechanisms with fluid driven actuators, *Mechanism and Machine Theory* 44(5): 1009 – 1018.
URL: *http://www.sciencedirect.com/science/article/B6V46-4SVM0W6-1/2/0ece208ab278bd053c985491f2e03d53*

[147] Zhang, X. & Ivlev, O. [2010]. Simulation of interaction tasks for pneumatic soft robots using simmechanics, *Robotics in Alpe-Adria-Danube Region (RAAD), 2010 IEEE 19th International Workshop on*, pp. 149 –154.